machines

MDPI

Article

Kinematic Modeling and Preliminary Field Evaluation of a Link-Driven Hopper Planting Mechanism for a 3.4 kW Walking-Type Pepper Transplanter

Eliezel Habineza [1,2], Md Razob Ali [2], Md Nasim Reza [1,2], Kyu-Ho Lee [1,2], Seok-Ho Park [3], Dae-Hyun Lee [1,2] and Sun-Ok Chung [1,2,*]

[1] Department of Smart Agricultural Systems, Graduate School, Chungnam National University, Daejeon 34134, Republic of Korea; eliezel.habineza@o.cnu.ac.kr (E.H.); reza5575@cnu.ac.kr (M.N.R.); leedh7@cnu.ac.kr (D.-H.L.)
[2] Department of Agricultural Machinery Engineering, Graduate School, Chungnam National University, Daejeon 34134, Republic of Korea; ali1999@o.cnu.ac.kr
[3] National Institute of Agricultural Science, Rural Development Administration, Jeonju 54875, Republic of Korea; shpark1827@korea.kr
* Correspondence: sochung@cnu.ac.kr; Tel.: +82-42-821-6712

Abstract

Labor shortages and reliance on manual seedling transplanting constrain pepper production from meeting market demand. To address this mechanization gap, the development of new agricultural machinery is an urgent priority. This study presented kinematic modeling and field validation of an automatic link-driven hopper planting unit for a 3.4 kW walking-type pepper transplanter under development. Kinematic behavior of the hopper was analyzed through mathematical modeling and dynamic simulation and validated under actual transplanting conditions under ridge-patterned field. The optimal design (crank length: 75 mm; 60 rpm) achieved a stable elliptical trajectory that enabled synchronized seedling pickup, tray release, and soil deposition while maintaining vertical alignment. Under this setup, the hopper followed a stable elliptical trajectory (166.88 mm × 318.81 mm), with supply and deposition coordinates of approximately (321 mm, −322 mm) and (293 mm, −617 mm), and peak velocities and accelerations within 0.47 m/s and 1.68 m/s^2, respectively. Field results showed that the proposed mechanism enabled reliable transplanting performance, achieving a mean planting depth of 27.06 ± 8.18 mm and an uprightness angle of 80.03 ± 7.56°, which fall within agronomic requirements for early pepper establishment. The overall defect rate was low (7.17 ± 3.73%), leading to a 92.83 ± 3.73% success rate at a throughput of 24 seedlings min^{-1}. Variety-dependent responses were observed: Kaltan seedlings exhibited lower defect rates and greater stability than Shinhung seedlings, highlighting the importance of plug strength and stem rigidity in automated systems. These results demonstrate that the mechanism supports fully automated transplanting with acceptable agronomic quality and provides practical design guidance for advancing mechanized pepper production.

Keywords: agricultural machinery; pepper transplanter; hopper-type transplanting mechanism; kinematic analysis

check for updates

Academic Editor: Alessandro Gasparetto

Received: 27 September 2025
Revised: 18 November 2025
Accepted: 18 November 2025
Published: 21 November 2025

Citation: Habineza, E.; Ali, M.R.; Reza, M.N.; Lee, K.-H.; Park, S.-H.; Lee, D.-H.; Chung, S.-O. Kinematic Modeling and Preliminary Field Evaluation of a Link-Driven Hopper Planting Mechanism for a 3.4 kW Walking-Type Pepper Transplanter. *Machines* **2025**, *13*, 1074. https://doi.org/10.3390/machines13121074

Copyright: © 2025 by the authors. Licensee MDPI, Basel, Switzerland. This article is an open access article distributed under the terms and conditions of the Creative Commons Attribution (CC BY) license (https://creativecommons.org/licenses/by/4.0/).

1. Introduction

Global demand for labor-efficient and high-precision agricultural technologies continues to intensify, particularly in vegetable production, where manual operations domi-

nate [1]. Among these, seedling transplanting is a repetitive, delicate, and time-sensitive task that poses significant challenges in terms of labor cost, consistency, and timeliness [2]. These constraints are especially evident in pepper (*Capsicum annuum* L.) cultivation, where the transplanting process directly influences plant establishment, growth uniformity, and yield potential [3,4].

In the Republic of Korea, the dominant practice for pepper transplanting involves the manual placement of seedlings into plastic-mulched, ridge-patterned fields, which ensures soil moisture conservation and weed suppression but also complicates mechanization due to the geometric and structural characteristics of the ridge fields [5]. While manual transplanting is effective for handling delicate seedlings, increasing unsustainability arises due to the aging rural workforce and seasonal labor shortages [6]. Consequently, the mechanization of seedling transplanting has emerged as a key research focus to boost planting efficiency, minimize transplanting errors, and support precision agriculture practices [7]. Persistent labor shortages, dependence on manual seedling transplanting methods, and the aging population engaged in farm work have significantly contributed to the decline in pepper production and cultivated areas in several countries, leading to production shortfalls and an inability to meet market demand [8]. The Republic of Korea experienced the farming population decreasing from 3.06 million in 2010 to 2.21 million in 2021, with 46% of farmers over 60 years old and 35% over 70, which led to pepper production falling from 117.8 to 92.8 thousand tons and shrank cultivation areas from 45.4 to 33.4 thousand hectares between 2013 and 2021 [9].

In 2022, the mechanization rate for pepper cultivation was 99.6% for tillage, 0% for planting, 54.0% for plastic mulching, 87.8% for pest control, and 0% for harvesting [10]. The seedling transplanting process operates through a synchronized sequence of supply, extraction, and planting mechanisms, commonly used in vegetable transplanters, in which the planting device moves vertically to receive seedlings from the supply unit and then releases them into the soil [11]. Various planting mechanisms are used in transplanters, including link-driven, wheel-driven, and gear-driven hoppers. The link-driven type employs interconnected linkages that allow relative motion for precise planting, the wheel-driven type uses wheels and roller guides to control hopper movement and facilitate opening and closing actions, while the rotary gear-driven type relies on a series of gears to transmit motion to the planting hoppers [12]. Among them, a mechanically driven link-based planting mechanism offers potential solutions for improving seedling placement accuracy and repeatability [13]. These mechanisms operate based on a series of interconnected mechanical links that translate rotary motion into complex spatial trajectories for planting hoppers [14]. Compared to other mechanisms such as gear-driven and wheel-driven types, link-driven designs offer greater flexibility in shaping the planting path and maintaining vertical seedling orientation, both critical for delicate crops like pepper. Moreover, they are relatively simple to fabricate, robust, and scalable for field operation [15].

A key challenge in designing such mechanisms lies in optimizing the planting trajectory to synchronize the seedling release point with the furrow position and minimize mechanical stress on the seedlings during deposition. Poorly tuned link mechanisms may cause mechanical shocks, shallow planting depths, or improper uprightness, all of which reduce transplanting success rates [16,17]. Kinematic modeling and simulation enable predictive analysis of transplanting device motions, ensuring optimal design parameters that enhance both mechanical efficiency and field performance [18]. The process involves creating mathematical models, simulating the motion of operational components, and conducting performance tests under field conditions based on agronomic traits [19]. Researchers have widely utilized these analyses to optimize the position, velocity, and acceleration of planting mechanisms, thereby enhancing design efficiency and achieving

high seedling planting success rates. A transplanting mechanism was designed [20] using planetary Bezier gears to increase the speed of potted seedling transplantation. A virtual prototype was simulated with commercial software, and seedling pickup experiments achieved a 98.2% success rate at 150 rpm carrier rotation. A kinematic model was developed [21] for a gear-driven rotary planting mechanism in a self-propelled onion transplanter. The simulation determined a maximum velocity of 1032 mm/s and an acceleration of 651 mm/s^2, while validation experiments revealed a power consumption of 35.4 W at 60 rpm, with transplanting rates of 60 and 120 seedlings per minute. Kinematic analysis was used [22] to optimize the motion trajectory of a seedling-picking and transplanting robot arm, achieving a 95.3% transplanting success rate.

Although several commercial vegetable transplanters exist, most are developed for flat-bed field structures and rely on rotary wheel- or gear-driven planting systems optimized for crops such as tomato, cabbage, or onion, rather than pepper. Despite notable advances in mechanized vegetable seedling transplantation [19–22], a gap remained in mechanically driven hopper transplanters explicitly designed and validated for pepper cultivation under ridge-type field conditions. These machines often lack compatibility with the narrow ridge geometry, steep sidewalls, and plastic-mulched surfaces commonly used in Korean pepper cultivation, resulting in misalignment, excessive disturbance to the ridge soil, or poor uprightness of the inserted seedling. Furthermore, commercially available systems typically demand heavier tractors, higher traction power, or pneumatic components, making them unsuitable for the small-scale, fragmented farms dominant in Korea [8,12]. High procurement and maintenance costs also limit adoption among smallholder growers [11]. Therefore, there remains a critical need for a compact and mechanically simplified link-driven planting device specifically designed to improve trajectory control, upright placement, and adaptability to plastic-mulched ridge fields in the Republic of Korea. This study addresses that gap by coupling kinematic modeling with ridge-field validation, quantifying tolerance-induced trajectory errors and phase-sensitive release performance for a link-driven hopper unit on a 3.4 kW walking-type platform.

Therefore, the objective of this study was to perform kinematic modeling and validate a link-driven hopper planting device for a 3.4 kW walking-type pepper transplanter prototype, capable of precisely placing seedlings upright with minimal mechanical complexity under ridge-patterned field conditions. The analysis focused on hopper position, velocity, acceleration, and trajectory to ensure smooth and reliable transplanting performance.

2. Materials and Methods

2.1. Structure of the Walking-Type Automatic Pepper Transplanter Under Development

A 3.4 kW single-row pepper transplanter prototype under development, equipped with a link-driven planting mechanism, was designed and evaluated in this study. Figure 1 provides an overview of the main components of the designed pepper seedling transplanter. A three-dimensional (3D) model of the walking-type automatic pepper transplanter, which comprises the seedling tray conveying, the seedling picking, and the link-driven hopper planting mechanisms, as shown in Figure 1i. The seedling picking mechanism consists of a pair of pins designed to automatically extract a single seedling from a 6 × 12 cell tray held in place by the tray conveyor. After extraction, the seedling is released into the hopper of the planting device. The planting device then deposits the seedling into the soil, while the molding wheel presses the soil around the base of the seedling to ensure good contact with the root zone through a fully synchronized and automated coordination of both transplanting mechanisms. The planting mechanism comprises key components, including a crank, coupler, rockers, connecting links, a hydraulic pipe, and a planting

hopper. These components were interconnected through multiple links, as illustrated in Figure 1ii.

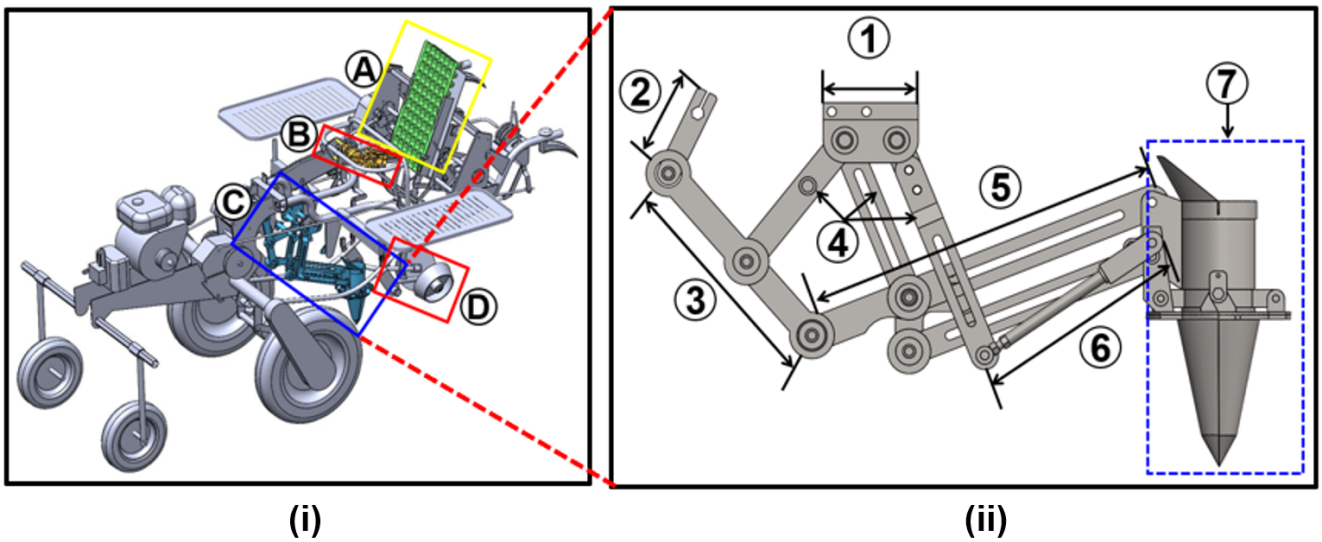


Figure 1. Overall structure of the pepper transplanter: (**i**) 3-D model of a 3.4 kW walking type automatic pepper transplanter: (A) tray conveyor, (B) seedling picking mechanism, (C) seedling planting mechanism, and (D) presser wheels; (**ii**) Major components of link-type planting mechanism: (1) ground link, (2) crank, (3) coupler, (4) rockers, (5) connecting link, (6) hydraulic pipe, and (7) hopper.

2.2. Working Principle of the Walking-Type Automatic Pepper Transplanter Under Development

The transplanter operates by starting the engine using a handle, steering with the handlebars, turning via the steering clutch, and engaging the transmission lever to initiate planting. The planting hopper is cone-shaped and inverted, equipped with two lateral springs that facilitate automatic opening and closing to receive seedlings from the supply mechanism and release them into the soil. The hydraulic pipe maintains the planting hopper in a vertical position, while the drive shaft transmits power to the crank, coupler, connecting link, and ultimately to the planting hopper. As the transplanter moves forward, the coordinated motion of multiple links guides the planting hopper along a predefined vertical trajectory. At the lowest position, the hopper flaps open to release the seedling into the soil. As the hopper rises, the flaps close, and the molding wheel simultaneously covers both sides of the planted seedling with soil, thereby completing the planting cycle in a continuous, automatic manner. Figure 2a illustrates the overall automatic seedling deposition principle of the pepper seedling transplanter, and Figure 2b shows the steps of automatic seedling deposition from the seedling tray to the hopper using an automatic picking mechanism.

2.3. Planting Mechanism Modeling

2.3.1. Agronomic Considerations for Mechanized Transplanting of Pepper Seedlings

The seedling planting mechanism was designed with consideration of the agronomic and physical characteristics of pepper seedlings, aiming to minimize mechanical damage while ensuring stable seedling delivery, proper spacing, and robust establishment in the soil. The concept involves accurately releasing seedlings into the planting hopper, forming a suitable planting furrow, placing the seedlings vertically into the furrow, and firming the soil around their roots to ensure stability and promote healthy growth [23]. Pepper seedlings are considered mature at 4 to 6 weeks of age, typically exhibiting 4 to 6 true leaves, a well-moistened root zone, and a sturdy stem measuring 2–3 mm in thickness and

10–15 cm in height [24]. Pepper seedlings should be maintained at a root zone moisture content of 50–70% to support healthy root development and planted at a depth of around 4 cm in soil with an optimal moisture content of 10–25% [5,25]. A commonly recommended spacing for pepper cultivation is 50–70 cm between rows and 40–60 cm between plants within a row, enabling balanced plant density, adequate air circulation, sufficient sunlight penetration, and convenient access for maintenance [26].

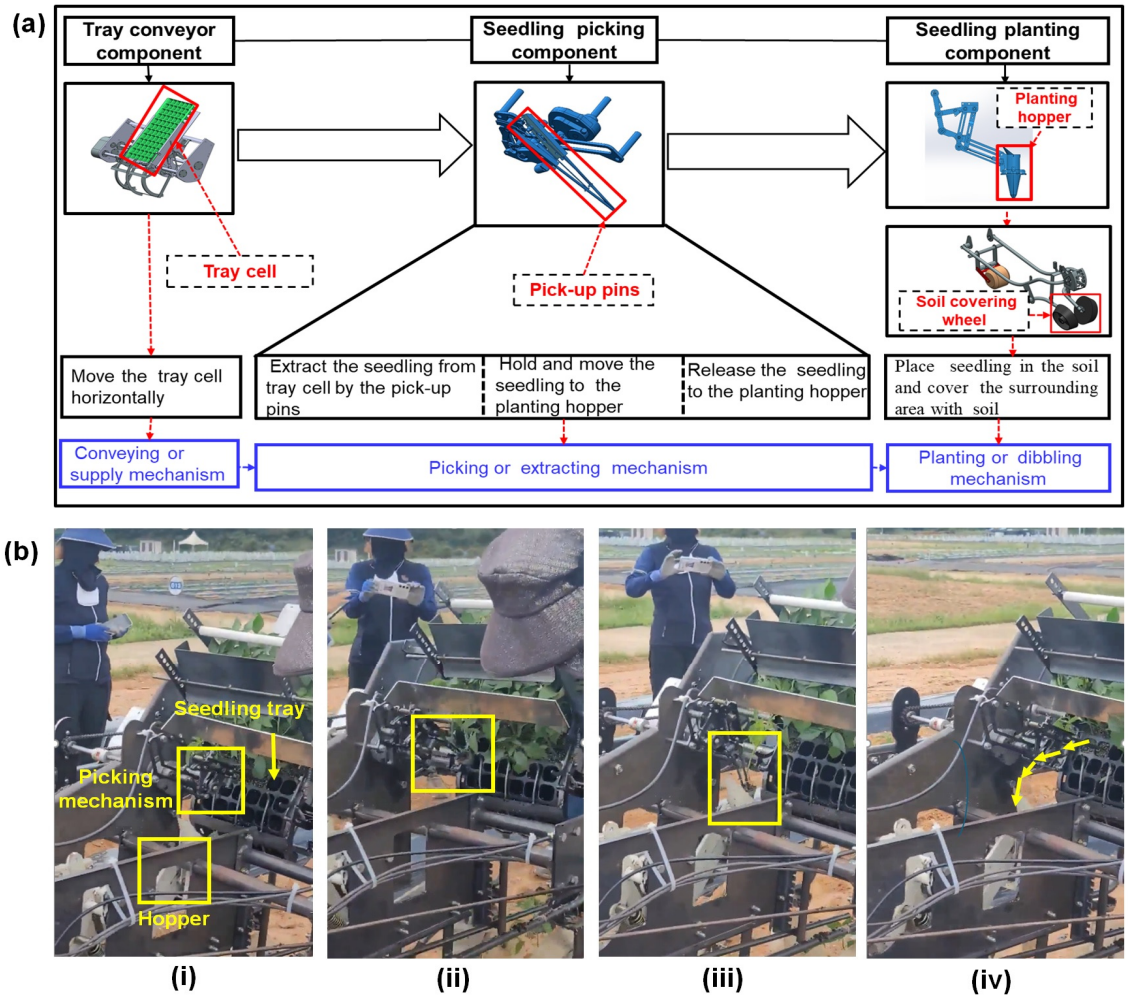


Figure 2. (**a**) A schematic overview of the automatic seedling transplanting process using the link-driven planting hopper of the transplanter under development, and (**b**) automatic seedling picking and release to the plating hopper: (i) Seedling tray, picking mechanism, and hopper position, (ii) seedling picking from tray, (iii) seedling deposition to the hopper, and (iv) seedling path from tray to the hopper through the picking mechanism.

In the Republic of Korea, pepper seedlings are planted in ridge-patterned fields that are covered with a 40 μm thick impermeable plastic film to minimize soil moisture extraction and control weed growth [5]. The ridge-patterned pepper field in Korea typically features a flat-top ridge design, with an inter-ridge distance of 1200 mm, a ridge width of 670 mm at the base, 470 mm at the top, a dam height of 230 mm, and a furrow width of 530 mm [27]. Figure 3 illustrates the structure of the pepper ridge-patterned field, and Table 1 provides the technical specifications of the pepper transplanter prototype.

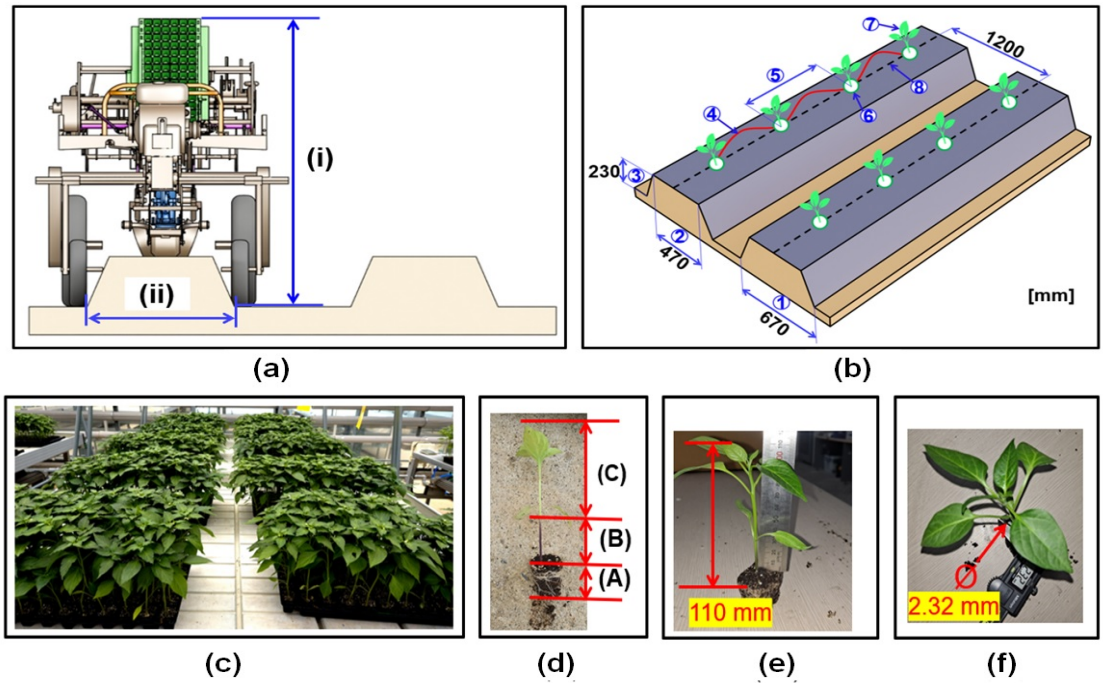


Figure 3. (**a**) Layout of transplanter in the field: (i) single row pepper transplanter, (ii) planting field; (**b**) Dimension of typical ridge-patterned field in Republic of Korea: (1) ridge width, (2) seedling bed width, (3) ridge height, (4) planting trajectory, (5) intra-row planting distance, (6) planting point, (7) seedling, and (8) planting row [5]; (**c**) Seedling seedlings in the trays, (**d**) Seedling characteristics and main parts of seedling: (A) root zone, (B) stem zone, and (C) leave zone; (**e**) Seedling height, and (**f**) Seedling stem thickness.

Table 1. Technical specifications of the link-driven hopper walking type pepper transplanter.

Item	Specification
Overall dimensions (Length × Width× Height/(mm))	2260 × 1410 × 1370
Weight (kg)	253
Rated power (kW (HP)/rpm)	3.4 (4.6)/1800
Cooling system	Air-cooled
Inclination (°)	±7
Engine cycle	4 strokes
Fuel type	Gasoline
Rated working speed (m/s)	0.23
Planting capacity (seeding/h)	1440
Number of operators	1

2.3.2. Structure of Links of the Planting Component

Figure 4 shows the structure of links and joints of the designed planting mechanism, and Figure 4a presents the dimensions of the links. The designed link-driven hopper planting device for planting pepper seedlings consisted of 11 main links arranged in four parts interconnected by 12 rotating joints to enable sliding or rotation during planting motion. The arrangements of links include 7 binary links (L_2, L_4, L_5, L_7, L_9, L_{10}, and L_{11}), the tertiary links (L_3, L_6, and L_8), and one ground link (L_1). The link structure in part 1 was made up of a crank (L_2), a coupler (L_3), a rocker (L_4), and a ground link (L_1) as shown in Figure 4b. Each link has the proper size to ensure smooth operation, and the connecting rod completes a 360° rotation for each planting cycle.

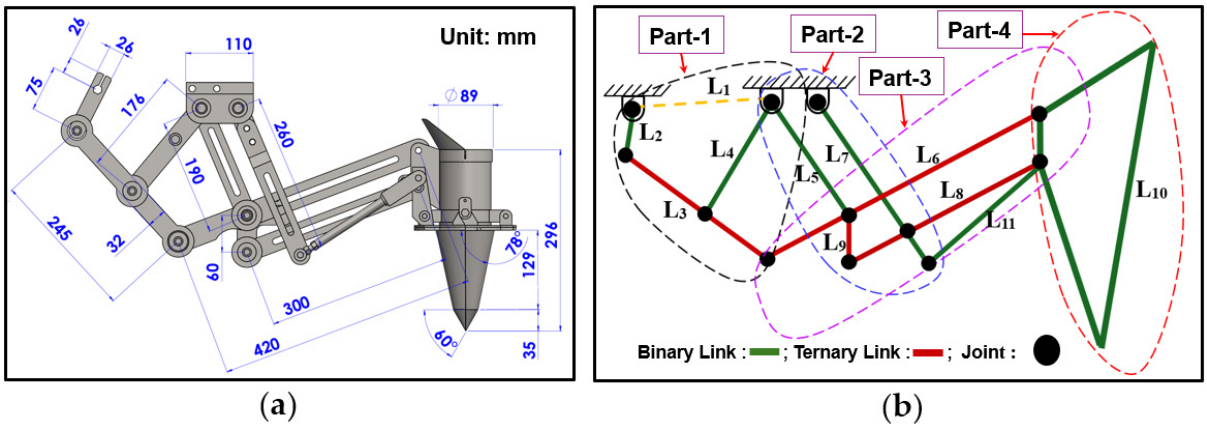


Figure 4. Structure of links and joints: (**a**) dimension of links and (**b**) configuration of links and joints.

The arrangement of links enables the hopper to follow the desired planting trajectory and to ensure the precise placement of seedlings in the planting furrow. The motion of the links is initiated from the crank, transmitted through the coupler, extended to the connecting links, and then reaches the planting hopper. The ground link (L_1) anchors the mechanism, while the crank (L_2) transfers rotational power from the gearbox to the coupler (L_3), which drives the rocker link (L_4) and the connecting link (L_6), ultimately transmitting motion to the hopper link (L_{10}). The rocker links (L_4, L_5, and L_7) follow the motion of the coupler link (L_3), allowing synchronized motion of the connecting links (L_6, L_8, L_9 and L_{11}) to move along a similar path while maintaining the upright position of the planting hopper link (L_{10}). The hydraulic pipe link (L_{11}) keeps the planting hopper moving up and down vertically, while the spring controls the opening and closing motion on the left and right sides of the hopper. Figure 5 illustrates the motion of the links of the link-type planting mechanism.

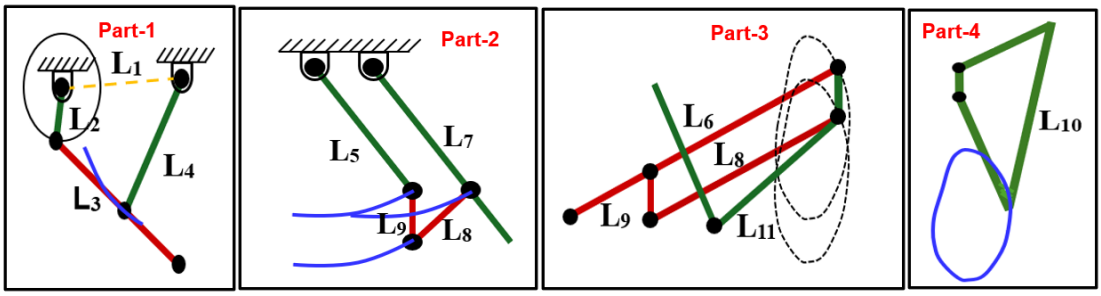


Figure 5. Configuration of links and joints of the proposed planting mechanism: Part 1: motion of crank and coupler links, Part 2: motion of rocker links, Part 3: motion of connecting links, and Part 4: motion of hopper.

2.3.3. Kinematic Modeling of the Link-Driven Hopper Using the Vector Loop Method

The motion of the link-driven planting hopper was analyzed to determine the optimal combination of link lengths, considering the positions of the main links, as shown in Figure 6. Mathematical equations were developed using the interior joint angles θ_2, θ_3, and γ for the main links L_1, L_2, L_3, and L_4, corresponding to a given crank angle θ_1. The trajectory path begins at the joint (O_1) of the crank link (L_2), propelling to the coupler link (L_3), which then transfers the power to the connecting link (L_6) and finally to the planting hopper. Where L_1 is the distance between fixed links (O_1 and O_2), L_2 is the length of the driving link- crank (O_1,A), L_3 is the length of the half coupler-link (AB), L_4 is the length of the rocker link (O_2, B), L_5 is the length of the rocker-link (O_2B), L_6 is the length of the part of the connecting link (CD), L_7 is the length of the link 5, S_1 is the length of relative distance

O_2A, S_2 is the length of relative distance O_2C, γ is the angle to S_1 in the triangle O_2BA, ω is the angle to S_2 in the triangle O_2BC, α_1 is the angle to L_4 in the triangle O_2CB, β_1 is the angle to L_7 in the triangle O_2CD, and θ_2 is the angle opposite to in triangle O_2O_1A.

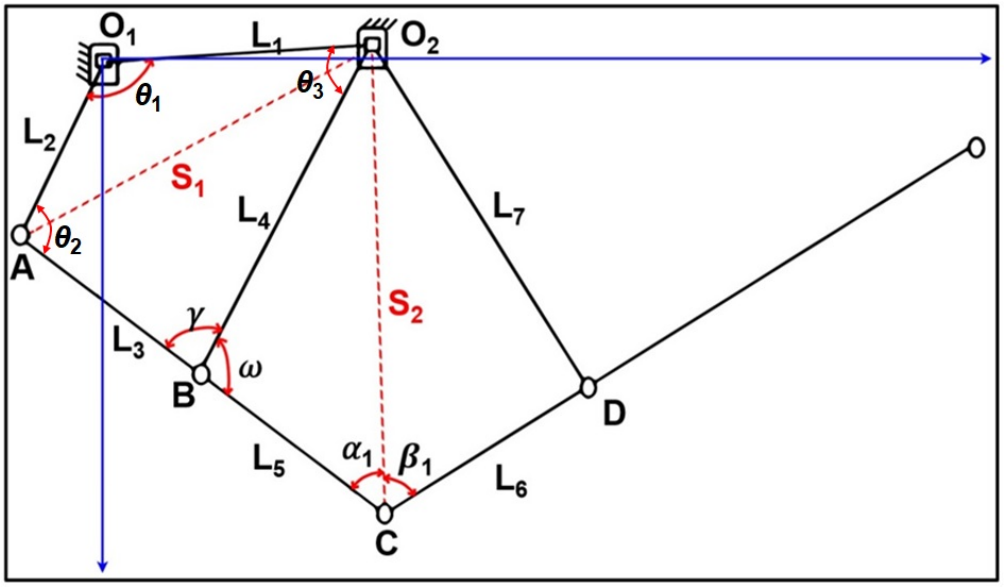


Figure 6. Kinematic representation of the link-driven hopper planting mechanism.

The vector loop equations for the position analysis of the link-driven hopper planting mechanism are presented in Equation (1). The corresponding kinematic values, velocity and acceleration can be obtained by taking the first and second derivatives of the position vector loop equations. Accordingly, Equations (2) and (3) represent the velocity and acceleration calculations, respectively.

$$\begin{cases} S_1 = \sqrt{L_1^2 + L_2^2 - 2L_1^2L_2^2cos\theta_1} \\ \gamma = cos^{-1}\left(\frac{L_3^2+L_4^2-S_1^2}{2L_3L_4}\right) \\ \omega = 180^\circ - cos^{-1}\left(\frac{L_3^2+L_4^2-S_1^2}{2L_3L_4}\right) \\ S_2 = \sqrt{L_4^2 + L_5^2 - 2L_4^2L_5^2cos\omega} \\ \beta_1 = cos^{-1}\left(\frac{L_6^2+S_2^2-L_7^2}{zL_6S_2}\right) \\ \alpha_1 = cos^{-1}\left(\frac{L_5^2+S_2^2-L_4^2}{2L_5S_2}\right) \end{cases} \quad (1)$$

$$\begin{cases} \omega_2 = -\omega_1\left[\frac{L_2sin(\theta_3-\theta_1)}{L_3sin\gamma}\right] \\ \omega_3 = -\omega_1\left[\frac{L_2sin(\theta_2-\theta_1)}{L_4sin\gamma}\right] \end{cases} \quad (2)$$

$$\begin{cases} \alpha_2 = \frac{\alpha_2L_2sin(\theta_2-\theta_4)+\omega_2^2L_2cos(\theta_2-\theta_4)-\omega_4^2L_4+\omega_3^2L_3cos(\theta_4-\theta_3)}{L_3sin(\theta_4-\theta_3)} \\ \alpha_3 = \frac{\alpha_2L_2sin(\theta_2-\theta_3)+\omega_2^2L_2cos(\theta_2-\theta_3)+\omega_3^2L_3-\omega_3^2L_4cos(\theta_4-\theta_3)}{L_3sin(\theta_4-\theta_3)} \end{cases} \quad (3)$$

The reception of seedlings from the supply mechanism and their placement in the planting furrow are synchronized with the opening and closing of the hopper. The earlier or delayed opening and closing of the planting hopper can result in defects, damage, or misplanting. To ensure planting precision, the hopper flaps must remain closed while

receiving seedlings and should open only after the vertical descent is complete. The seedling is dropped from the supply mechanism at the highest point of its trajectory and is released into the planting furrow once the hopper reaches the appropriate position. The process is controlled by the motion of the hydraulic pipe and spring, driven by power from the gearbox through the crankshaft. The motion of the connecting link lifts and closes the hopper to receive the seedling by applying force on the hydraulic pipe. Once the seedling is received, the hopper moves downward, opening the flaps to release it into the soil. The compressed spring restores the flaps to their closed position, making them ready for the next seedling. Simulation trials with crank lengths ranging from 65 mm to 85 mm were conducted to determine the optimal length that ensures proper downward and upward positioning of the hopper. The timely opening and closing of the planting hopper, along with the corresponding contraction and extension lengths of the hydraulic pipe spring, and the relationship between the applied forces, can be calculated using Equations (4)–(8) as follows:

Hydraulic pipe force can be expressed as Equation (4):

$$F_h = P \times A \tag{4}$$

Spring force (Hooke's Law) can be expressed as Equation (5):

$$F_s = k \times x \tag{5}$$

Hydraulic pipe length relation: the extension or contraction of the hydraulic pipe is proportional to the hydraulic force applied.

$$L_h = L_{h0} \ + \Delta L_h \tag{6}$$

Spring length relation: the extension or contraction of the spring is related to the displacement.

$$L_s = L_{s0} \ + \Delta L_s \tag{7}$$

At the equilibrium condition for the hopper to open or close, the forces from the hydraulic pipe and the spring must balance, and the displacement of the spring can be expressed in terms of the length of the hydraulic pipe as Equation (8).

$$\begin{cases} F_h = F_s \\ P \times A = k \times x \\ x = \Delta L_h \end{cases} \tag{8}$$

where L_h: final length of the hydraulic pipe, L_{ho}: initial length of the hydraulic pipe, ΔL_h: change in length due to hydraulic force; *Ls*: final length of the spring, *Lso:* initial length of spring, ΔL_s: change in length due to spring force; F_h: force exerted by the hydraulic cylinder, *Fs*: force exerted by the spring, k: spring constant, x: extension or compression of the spring from the natural length, P: hydraulic pressure, and A: cross-sectional area of the hydraulic pipe. Figure 7 illustrates the opening and closing mechanism of the hopper.

2.4. Simulation and Validation Procedures

The planting mechanism, as a crucial component of the transplanter, was evaluated through virtual simulations to ensure the required position and trajectory of the hopper for the successful transplanting of pepper seedlings. A 3D dynamic model of the link driven hopper mechanism was developed using a commercial mechanical simulation software (SOLIDWORKS 2018, Dassault Systems SolidWorks Corp., Waltham, MA, USA) to evaluate the planting trajectory consistency during the rotation crankshaft, the maximum upward position for receiving seedlings, and the downward position for accurate placement in the

planting furrow. During the transplanting process, power is applied to the crankshaft from the engine, which drives the main links of the planting device, enabling the hopper to move upward and downward in an oval trajectory. The rotational motion of the hopper enables it to capture seedlings from the supply mechanism and advance with the transplanter in a scalloped pattern, ensuring the vertical placement of seedlings into the soil. Simulation parameters, including fixed and variable conditions, are summarized in Table 2. For the simulation, steel alloy 1020 was selected for both the body cover and other components of the planting device due to its strength and durability, making it well-suited for agricultural field conditions. The physical properties of steel alloy 1020 include a density of 7.85×10^3 kg/m^3, a modulus of elasticity of 207 GPa, a Poisson's ratio of 0.3, and a yield strength of 210 MPa. Figure 8 illustrates the simulation procedures for the link-driven hopper planting mechanism using commercial software.

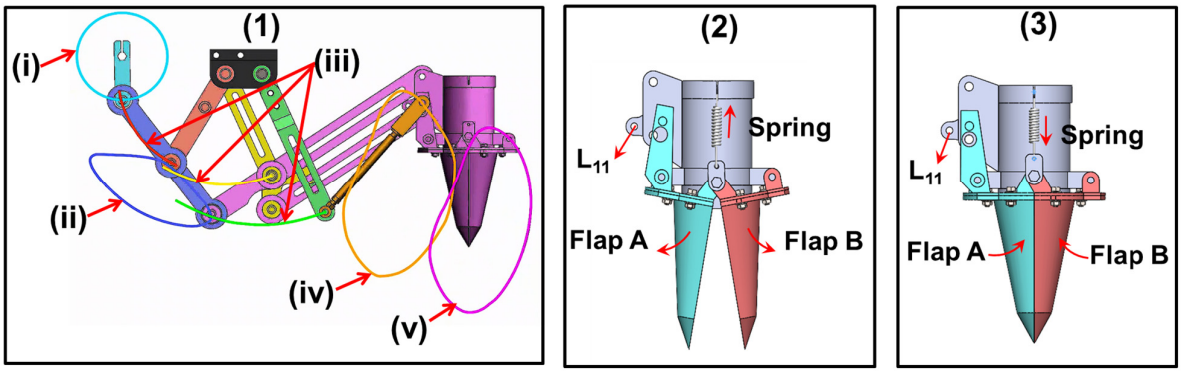


Figure 7. Opening and closing mechanism of the hopper: (**1**) Motion trajectory of main links: (i) trajectory of crank, (ii) trajectory of coupler, (iii) trajectory of 3 rocker links, (iv) trajectory of hydraulic pipe, and (v) trajectory of hopper, (**2**) Hopper opening, and (**3**) Hopper closing.

Table 2. Parameters used in the simulation of the planting mechanism.

Type of Parameter	Details
Fixed parameters	Lengths of main links (couplers, rockers, and connecting links) Forward speed Planting interval
Variable parameters	Length of crankshaft Rotational speed of the mechanism

For the validation, a field test was conducted in September 2024 at the experimental field (Lat. 35.84° N, Long. 127.13° E) of the National Institute of Agricultural Sciences, Rural Development Administration (RDA), Jeonju, Republic of Korea. Figure 9 shows the location of the experimental site, including the layout of the field used for testing and the ridge pattern with mulched beds where pepper seedlings were transplanted. A tractor-drawn soil-lifting, hill-covering, and plastic mulching machine was used to make the standard mechanized cultivation method and to cover the ridges with plastic mulch film. The single-row pepper transplanter prototype equipped with a link-driven planting mechanism was used for the field test using a 72-cell tray for the automatic transplanting of pepper seedlings. According to the USDA soil texture classification, the field soil was classified as sandy loam with a moisture content of 23.68% as shown in Table 3.

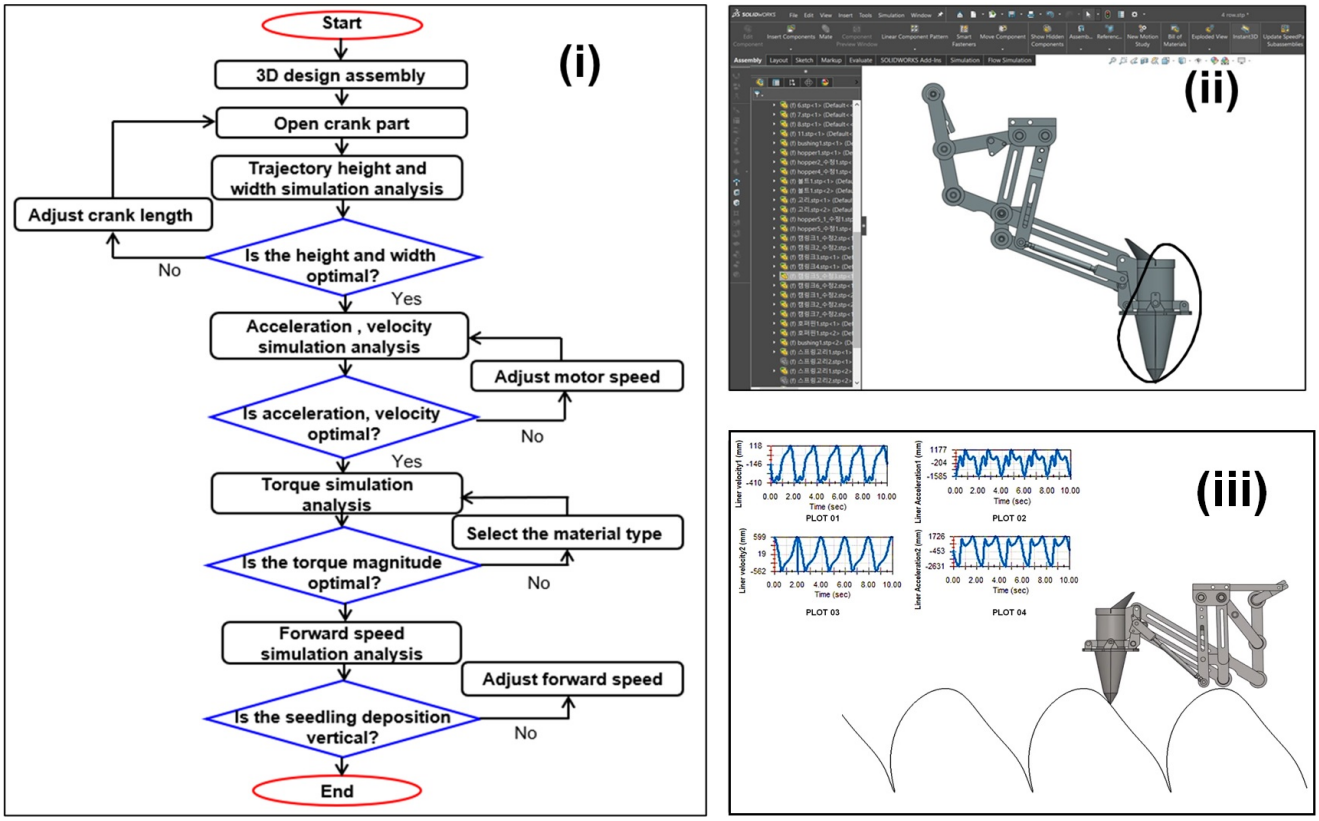


Figure 8. Simulation procedures: (**i**) simulation flowchart, (**ii**) trajectory of the end-hopper in static motion, and (**iii**) trajectory of the end-hopper in dynamic motion.

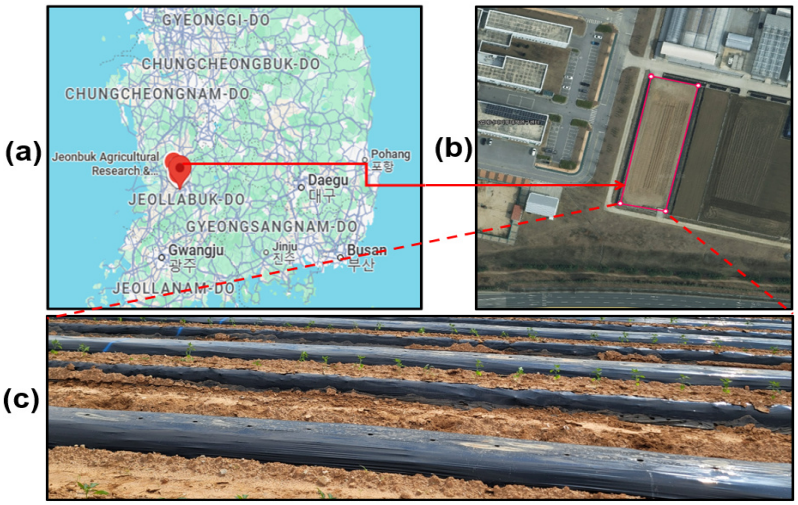


Figure 9. Experimental site: (**a**) field location, (**b**) experimental field, and (**c**) planting ridge.

Table 3. Major soil properties of the experimental field.

Sample	Soil Water Content (%)	Soil Temperature (°C)	Cone Index (MPa)	Soil EC (dS/m)	Bulk Density (g/cm^3)	Soil Texture		
						Sand	Silt	Clay
Soil	23.68 ± 0.61	28.6 ± 0.4	0.74 ± 0.05	0.34 ± 0.00	1.45 ± 0.08	69.6%	20.0%	10.4%
						Sandy loam		

During the validation process, a triaxial accelerometer (Model 356A15; PCB Piezotronics Inc., Depew, NY, USA) was mounted at the endpoint of the planting hopper to capture

acceleration variations. Data acquisition was facilitated using a four-channel dynamic signal acquisition module (Model NI 9234; National Instruments, Austin, TX, USA), connected to an eight-slot USB Compact DAQ chassis (Model NI cDAQ-9178; National Instruments, Austin, TX, USA). A custom program developed in LabVIEW (Version 2018; National Instruments, Austin, TX, USA) was employed to collect acceleration signals. The system operated at a sampling frequency of 1000 Hz, with each data block spanning 10 s. The detailed specifications of the acceleration measurement instruments are summarized in Table 4.

Table 4. Specifications of acceleration measurement instruments used in the experiment.

Item	Model	Specification
Acceleration sensor	356A15	Sensitivity (±10%): 10.2 mV/(m/s^2) Measurement range: ±490 m/s^2 Frequency range (±10%): 1.4–6500 Hz Resonant frequency: ≥25 k Broadband resolution: 0.002 m/s^2 rms
Connector cable	C4P5M3BP	Shielded, lightweight, FEP cable 4-socket plug, IP68 rated to triple splice assembly with (3) 1 ft coaxial cables each with a BNC plug (AC)
Data acquisition device	NI cDAQ 9188	Timing accuracy: 50 ppm of sample rate Timing resolution: 12.5 ns Internal base clocks: 20~100 kHz Regeneration: 1.6 MSs^{-1}
Software	LabVIEW 2020	NI Instrument Professional development system (64-bit) for Windows NI recommends 1 GB of RAM (min.)

Velocity data were subsequently derived through numerical integration of the measured acceleration. Peak linear velocities and accelerations of the link-driven hopper planting mechanism were evaluated under various trial conditions at an operational speed of 60 rpm. To track hopper movement, a high-resolution video (1280 × 720 pixels, 24 fps) was analyzed using open-source video-based tracking software to extract frame-wise displacement motion. Additionally, Figure 10 presents a schematic diagram of the data acquisition system, a photograph of the data acquisition unit, and the sensor placement configuration. Table 5 summarizes the validation parameters during the field test.

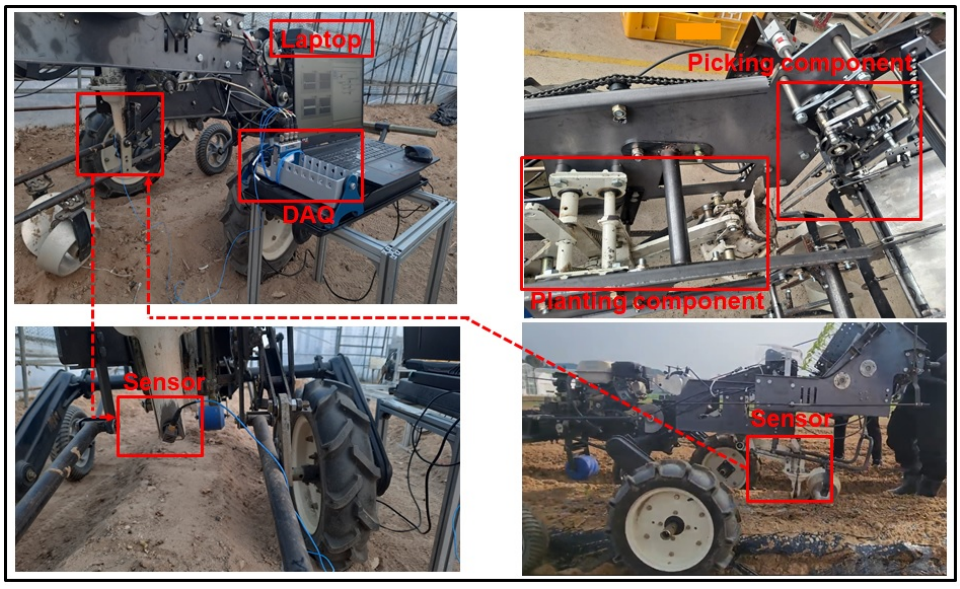


Figure 10. Schematic diagram of the sensors setup during the data acquisition process.

Table 5. Parameters used in the field test validation of the planting mechanism.

Parameter	Value	Unit
Forward operating speed	0.23	m/s
Crank rotational speed	60	rpm
Theoretical planting spacing	400	mm
Ridge width	0.67	m
Seedling bed width	0.47	m
Mulch film thickness	40	μm
Seedling age	6	week
Tray type	72-cell (6 × 12)	–
Soil moisture	23.68 ± 0.61	% (w.b.)
Planting position	Center ridge, single-row	–

2.5. Field Performance of the Prototype Transplanter

Two red pepper varieties with similar growth requirements, Kaltan and Shinhung, were selected for the field test across 12 experimental plots. Each variety was grown in six trays and planted alternately every three trays, as shown in Figure 11. At the time of transplanting, the seedlings were six weeks old. Kaltan seedlings were transplanted from trays 1, 2, 3, 7, 8, and 9, while Shinhung seedlings came from trays 4, 5, 6, 10, 11, and 12. The test field featured a mechanized cultivation pattern with mulched ridges measuring 30 m in length and 0.67 m in width. Each ridge included a 0.47-m-wide seedling bed covered with 40 μm thick black plastic mulch film. The transplanter was operated at a forward speed of 0.23 m/s, maintaining an intra-row planting spacing of approximately 400 mm. To assess planting performance, the seedling defect rate, average upright angle, and average planting depth were evaluated using Equations (9)–(11) as provided below.

$$\text{Defect rate}(\%) = \left(\frac{\text{Number of defective seedlings}}{\text{Total number of transplanted seedling}}\right) \times 100 \quad (9)$$

$$\text{Upright angle}(^\circ) = \left(\frac{\text{Summation upright angles}}{\text{Total number of transplanted seedling}}\right) \quad (10)$$

$$\text{Planting depth}(\text{mm}) = \left(\frac{\text{Summation of depth of holes}}{\text{Total number of transplanted seedling}}\right) \quad (11)$$

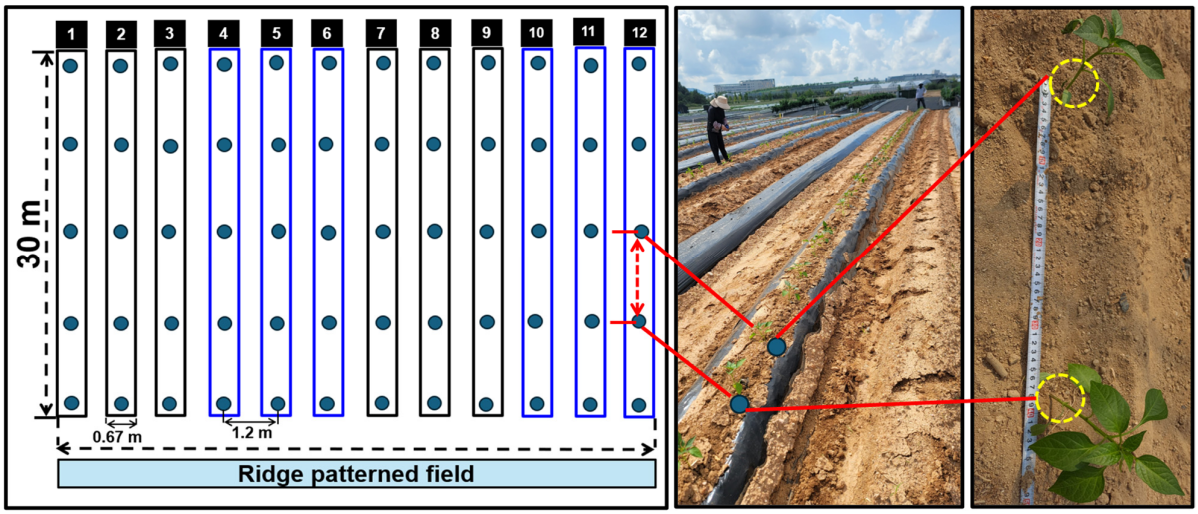


Figure 11. Experimental plot layout: black color for Kaltan (trays 1–3, 7–9), and blue for Shinhung (trays 4–6, 10–12).

To evaluate planting performance, measurements were taken at three randomly selected sections in the test plot, with 10 transplanted seedlings assessed per section (n = 31). Defected seedlings were visually inspected and counted based on criteria such as those with issues such as improper planting depth, misalignment, or being completely laid down outside the planting hole. The planting depth of a seedling refers to the vertical distance from the soil surface to the base of the seedling after transplantation into the main field. Planting depth was measured using a steel tape ruler (model: DWHT36337L; Stanley Black & Decker, Baltimore, MD, USA) with 1 mm accuracy, from the soil surface to the bottom of the planting hole immediately after deposition to avoid soil disturbance effects. Seedling planting angle (uprightness) refers to the vertical position of the seedlings after transplantation, whereas the total number of transplanted seedlings indicates the overall count of all seedlings transplanted using the transplanter. The uprightness was quantified using a protractor (model: K-1500; KORING Co., Ltd., Paju, Republic of Korea) with ±0.1° resolution, measuring the deviation from the vertical axis by placing the reference edge along the seedling stem approximately 1 cm above the soil surface. Stem diameter was measured using a digital caliper (model: 201-150P; Jongwon Tooling Co., Ltd., Seoul, Republic of Korea) with ±0.01 mm accuracy on the same height reference point. Table 6 shows the measurement summary with the measuring instruments specifications used during the study. All measurements were conducted by trained operators to ensure consistency, and three repeated measurements were taken when anomalies were suspected. Assessment procedures followed commonly accepted transplanting evaluation standards to ensure reliable and repeatable field validation. Figure 12 illustrates the measured parameters related to transplanting performance.

Table 6. Measurement instruments and accuracy used for field performance evaluation.

Measurement Parameter	Instrument Used	Model/Type	Measurement Accuracy/ Resolution	Reference Location on Seedling/Field
Defected seedlings	Visual inspection	–	Qualitative	Whole plant after release
Planting depth	Steel tape ruler	Standard, metric	1 mm accuracy	From soil surface to bottom of planting hole
Planting angle (uprightness)	Angle ruler	Protractor type	±0.1° resolution	~1 cm above soil surface along stem
Stem diameter	Digital caliper	Vernier type	±0.01 mm resolution ±0.01 mm accuracy	~1 cm above soil surface on stem

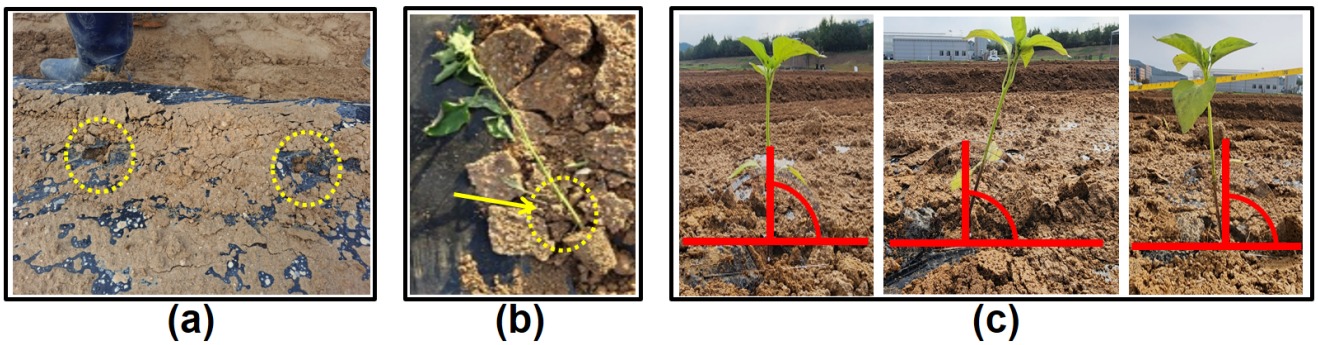


Figure 12. Measured transplanting performance parameters: (**a**) planting holes, (**b**) defective seedlings, and (**c**) uprightness of the seedlings.

3. Results

3.1. Position of the Planting Hopper

Considering the rotational motion of the link-driven hopper planting mechanism, five simulation trials were conducted to analyze the trajectory of the planting hopper

under varying crank lengths ranging from 65 mm to 85 mm. The primary link dimensions included a coupler of 245 mm, three-rocker links of 176 mm, 190 mm, and 260 mm, and two connecting links of 420 mm and 300 mm. The hopper length was maintained at 296 mm across all trials to align with the standard hopper length for single-row transplanters [28]. Each trial represented a unique kinematic configuration. As shown in Figure 13, the hopper positions during the seedling supply and deposition phases are indicated by labels (a_1) to (a_5) and (b_1) to (b_5), respectively. In these illustrations, the yellow bullet marks the location of the hopper at the seedling supply point, the black dot indicates the seedling position inside the hopper, and the blue bullet represents the planting hole. Accurate alignment of the seedling with the centers of the yellow and blue bullets defines the appropriate positioning for both collection and deposition phases.

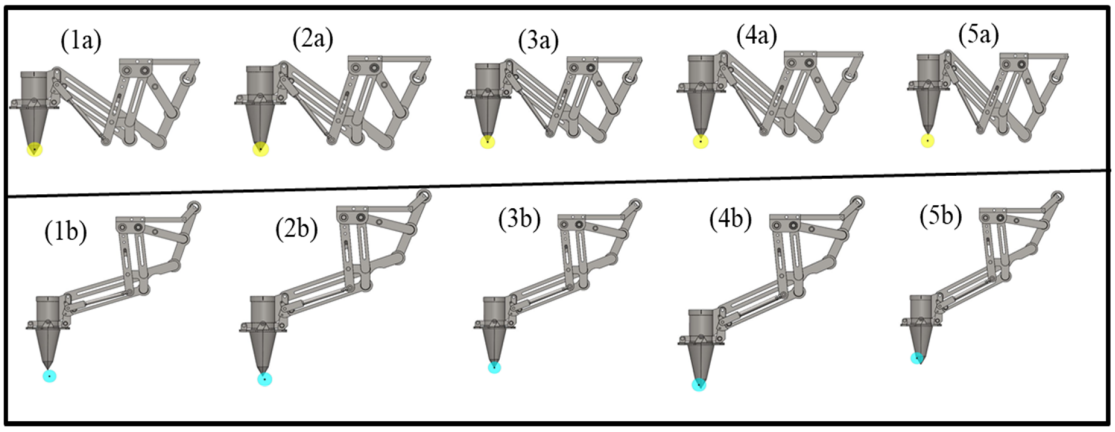


Figure 13. Simulated positions of the planting hopper at various crank lengths: (1a–5a: position of the hopper during seedling supply) and (1b–5b: position of the hopper during seedling deposition).

The seedling supply and deposition points varied with crank length. As shown in Table 7, the motion of the hopper at the seedling supply point ranged from 317.97 mm to 322.49 mm along the *X*-axis and from −310.10 mm to −342.09 mm along the *Y*-axis. At the deposition point, the hopper moved within the range of 282.15 mm to 296.99 mm along the *X*-axis and −643.57 mm to −592.94 mm along the *Y*-axis. The planting trajectory width spanned from 143.03 mm to 191.66 mm, while the trajectory height ranged from 273.10 mm to 366.81 mm. Among the five trials, a crank length of 75 mm was found to be optimal for ensuring proper seedling collection and deposition while preventing mechanical damage to the stems and leaves. This configuration yielded a planting trajectory width of 166.88 mm and a height of 318.81 mm, with seedling supply and deposition positions at 320.682 mm, −321.56 mm, 292.63 mm, and −617.28 mm along the *X*- and *Y*-axes, respectively. Larger or smaller crank lengths resulted in deviations from the desired oval trajectory, leading to improper seedling placement within the seedling cup or planting furrow. To evaluate the reliability and predictive capability of the simulation model, a comparison was made between the simulated and experimentally measured positions of the hopper. The assessment focused on identifying the maximum positional coordinates of the hopper during both the seedling supply and soil deposition phases. According to the simulation results, the maximum hopper position at the seedling supply stage was recorded at 320.68 mm along the *X*-axis and −321.56 mm along the *Y*-axis. Experimental observations showed a maximum supply position of 223.67 mm along the *X*-axis and −326.32 mm along the *Y*-axis. The discrepancy of approximately 97 mm in the X-direction is likely due to mechanical deflection, speed variation, linkage clearance, joint tolerance, assembly errors, and surface interaction forces that were not explicitly modeled.

Table 7. Simulated hopper positions and trajectory parameters for various crank lengths.

Combination	Crank Length (mm)	Seedling Supply Point		Seedling Deposition Point		Planting Trajectory	
		X-Axis (mm)	*Y*-Axis (mm)	*X*-Axis (mm)	*Y*-Axis (mm)	Width (mm)	Height (mm)
1.	65	322.49	−342.09	296.99	−592.94	143.03	273.10
2.	70	321.75	−331.75	295.82	604.92	154.89	295.73
3.	75	320.68	−321.56	292.63	−617.28	166.88	318.81
4.	80	319.42	−311.31	289.43	−630.13	179.20	342.46
5.	85	317.97	−310.10	282.15	−643.57	191.66	366.81

For the deposition phase, the simulation predicted a maximum position of 292.63 mm on the *X*-axis and −617.28 mm on the *Y*-axis, while the corresponding experimental values were 390.55 mm and −645.67 mm. The *Y*-axis predictions closely matched the experimental values; however, a greater deviation was observed along the *X*-axis, likely due to dynamic instability and linkage backlash at higher crank speeds.

The optimal path generated from the simulation was validated through field experiments. During simulation, the optimal planting-shaft rotational speed that produced the desired trajectory was 60 rpm; the same speed was used during actual pepper seedling planting. Table 8 presents the comparison between the simulated and experimental measured position of the hopper, while Figure 14 illustrates the simulated and experimental path trajectories of the end-hopper.

Table 8. Comparison between calculated and experimental measured maximum hopper positions.

Coordinates	Maximum Position of Hopper at Seedling Supply		Maximum Position of Hopper at Soil Deposition	
	X-Axis (mm)	*Y*-Axis (mm)	*X*-Axis (mm)	*Y*-Axis (mm)
Calculated	320.68	−321.56	292.63	−617.28
Measured	223.67	−326.32	390.55	−645.67

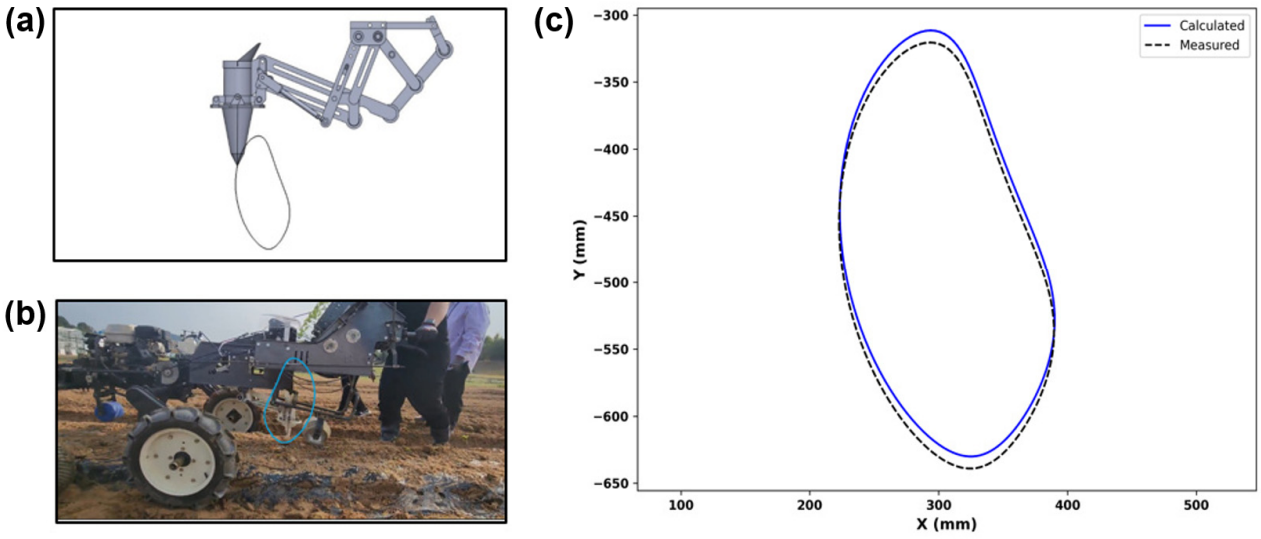


Figure 14. Positions of the planting hopper: (**a**) calculated position, (**b**) measured position, and (**c**) comparison of calculated and measured positions of the hopper.

3.2. Velocity, Acceleration, and Required Power

Each planting cycle lasted approximately 2.5 s, corresponding to one full rotation of the crankshaft as shown in Figure 15. The lengths of the main links were as follows: 75 mm for the crank link; 245 mm for the coupler link; 176 mm, 190 mm, and 260 mm for the three-rocker links; and 420 mm and 300 mm for the two connecting links. Simulated peak velocities ranged from +0.06 to −0.35 m/s (X) and +0.47 to −0.45 m/s (Y), showing balanced

bidirectional motion in both axes. During the experimental measurements, the peak velocities ranged from +0.43 to −0.63 m/s along the *X*-axis and from +0.95 to −0.80 m/s along the *Y*-axis. No velocity was observed along the *Z*-axis during the simulation. These velocity values fall within the typical target range for automated transplanting operations, which extends from 200 to 1032 mm per second, as reported by previous researchers such as [29]. The results confirm that the designed mechanism operates within the acceptable velocity range required for effective seedling transplanting. Figure 15 shows the temporal velocity variation in the hopper in both directions. The blue line indicates experimental data derived from accelerometer integration, while the red dashed line shows simulation output. Table 9 shows the comparison between the measured and calculated velocity of the planting hopper.

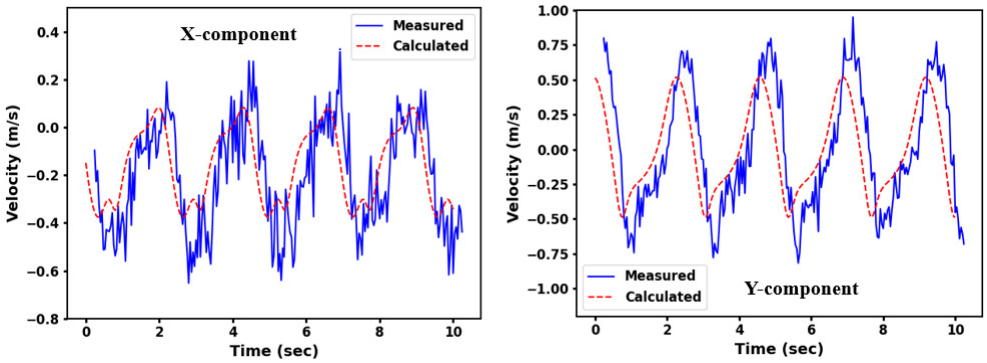


Figure 15. Simulated and experimental velocity curves in the *X*-and *Y*-axes.

Table 9. Comparison of measured and calculated velocity of the hopper.

Direction	Calculated (m/s)	Measured (m/s)
X-Component	+0.06 to −0.35	+0.43 to −0.63
Y-Component	+0.47 to −0.45	+0.95 to −0.80

The operational time used for both the experimentally measured and calculated accelerations was consistent with that applied in the velocity analysis. Figure 16 illustrates the peak calculated and measured accelerations along the *X*- and *Y*-axis directions. In the simulation, the maximum accelerations ranged from +0.75 to −0.95 m/s^2 along the *X*-axis and from +1.10 to −1.68 m/s^2 along the *Y*-axis. Experimentally, the corresponding peak accelerations ranged from +1.14 to −1.21 m/s^2 along the *X*-axis and from +1.61 to −2.65 m/s^2 along the *Y*-axis. No acceleration was detected along the *Z*-axis during the simulation, indicating that the hopper motion was primarily confined to a planar trajectory. As shown in Figure 16 and Table 10, both the measured and calculated acceleration profiles exhibited similar dynamic trends in the *X*- and *Y*-components, confirming strong agreement between simulation and experimental results. The measured accelerations showed slightly greater amplitude variations than the calculated values, particularly in the *Y*-direction, likely due to field conditions, joint mechanical tolerances, and surface irregularities during operation. Despite these minor discrepancies, the overall waveform patterns and frequency responses between the two datasets. These values were evaluated with reference to previous studies that reported the acceleration requirements for automated transplanting systems, typically ranging from 6501 to 8664 mm/s^2, as reported by [21]. Although the measured acceleration values in this study fall below the upper operational limits, they indicate a dynamically stable response of the mechanism under the tested conditions.

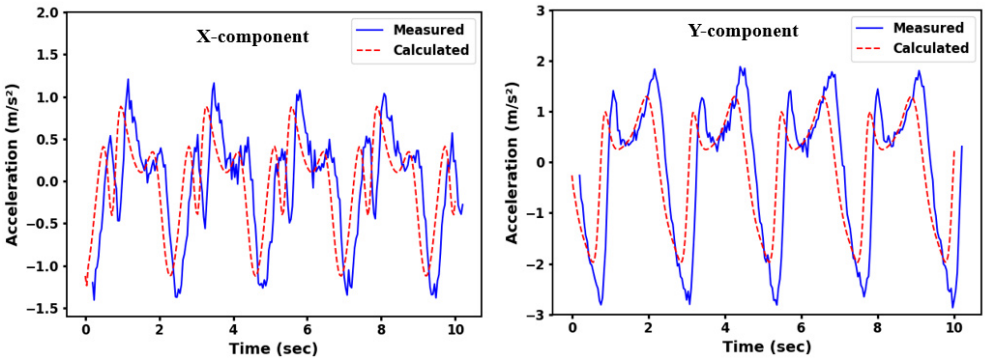


Figure 16. Calculated and measured acceleration curves in the *X*- and *Y*-axis.

Table 10. Comparison of measured and calculated acceleration of the hopper.

Direction	Calculated (m/s^2)	Measured (m/s^2)
X-Component	0.75 to −0.95	+1.14 to −1.21
Y-Component	+1.10 to −1.68	+1.61 to −2.65

During the transplanting process, the required input power was recorded for both simulation and field experiments as shown in Table 11. The maximum and minimum power ranged from +73.32 to −75.47 W and from +69.46 to −76.23 W for experimentally measured, respectively. Several studies have reported power requirements for vegetable seedlings transplanters. A study by [30] compared the consumed power of cam and four-bar-link semi-automatic vegetable transplanters. This study suggests that the recommended power requirement for vegetable seedling transplanters typically falls within the range of 50 W to 150 W, depending on the design and operational conditions. Power consumption observed in both simulation and experimental settings for pepper seedling transplanter prototype aligns well with the recommended power ranges reported in the literature for vegetable seedling transplanters. This alignment validates the efficiency and suitability of your transplanter design for practical agricultural applications.

Table 11. Power consumption of the planting component during the transplanting operation.

Parameter	Calculated (W)	Measured (W)
Power range	+73.32 to −75.47	+69.46 to −76.23

3.3. Seedling Deposition Performance

Transplanting seedlings from the nursery tray to the main field without proper care can lead to significant losses, including high mortality rates, poor establishment, and weak crop development. Excessive mechanical force during planting may cause stem fracture, leaf breakage, or root tearing, especially under poor synchronization conditions. Additionally, improper planting depth and incorrect seedling orientation are common causes of seedling defects [4]. Shallow planting can lead to seedling desiccation, while excessive soil coverage may restrict root respiration and hinder growth [16].

A total of 12 trays (six per variety) were used to evaluate the seedling defect rate across all transplanted seedlings. For upright angle and planting depth measurements, six representative trays (three per variety) were selected for detailed assessment, following standard transplanting evaluation procedures to ensure statistical independence and prevent pseudoreplication. During the field testing, a total of 864 seedlings (12 trays × 72 cells per tray; six trays per cultivar) were assessed for physical and positional damage across two pepper cultivars, Kaltan and Shinhung, as presented in Table 12. Each tray was treated as an experimental unit to avoid pseudoreplication, and tray-level percentages were used to calculate the mean defect and success rates with their corresponding standard deviations

(SD). The defect rate, representing the proportion of seedlings that were either physically damaged or failed to establish after transplantation, ranged from 2.77% to 8.33% for Kaltan and 4.16% to 13.88% for Shinhung. The mean defect rate of Kaltan (5.09 ± 2.27%) was notably lower than that of Shinhung (9.26 ± 3.90%), showing a 4.17 percentage-point difference. Correspondingly, the success rate was higher for Kaltan (94.91 ± 2.27%) than for Shinhung (90.74 ± 3.90%), indicating greater uniformity and transplanting stability in Kaltan seedlings. Figure 17 illustrates the distribution of transplanting performance. Kaltan shows a lower median defect rate with a narrower spread, while Shinhung exhibits a higher median defect rate and larger variability. A two-sample *t*-test ($t = -2.26$, $p = 0.053$, F = 2.94) showed that the difference was not statistically significant at $\alpha = 0.05$, although it was borderline significant. The wider variability observed in Shinhung implies greater sensitivity to mechanical or environmental stress factors during transplanting, whereas Kaltan demonstrated superior plug integrity and mechanical compatibility. The relatively small differences in standard deviations observed in both varieties indicate moderate variability and consistent transplanting outcomes. Furthermore, an analysis of variance (F-test) revealed a variance ratio of 2.94 between the two cultivars, suggesting that Shinhung exhibited significantly greater variability in defect rate compared to Kaltan.

Table 12. Defected seedlings during the transplanting process.

Seedling Variety	(6 × 12 Tray Cell)	Defected Seedlings	Defect Rate (%)	Success Rate (%)
Kaltan	Tray 1	5	6.94	93.06
	Tray 2	4	5.55	94.45
	Tray 3	2	2.77	97.23
	Tray 7	2	2.77	97.23
	Tray 8	3	4.16	95.84
	Tray 9	6	8.33	91.67
	Total (Ave. + SD)		5.09 ± 2.27%	94.91 ± 2.27%
Shinhung	Tray 4	3	4.16	95.84
	Tray 5	6	8.33	91.67
	Tray 6	8	11.11	88.89
	Tray 10	9	12.50	87.50
	Tray 11	10	13.88	86.12
	Tray 12	4	5.55	94.45
	Total (Ave. + SD)		9.26 ± 3.90%	90.74 ± 3.90%
	t-test		$t = -2.26$	$p = 0.0532$
	F-test		2.94	

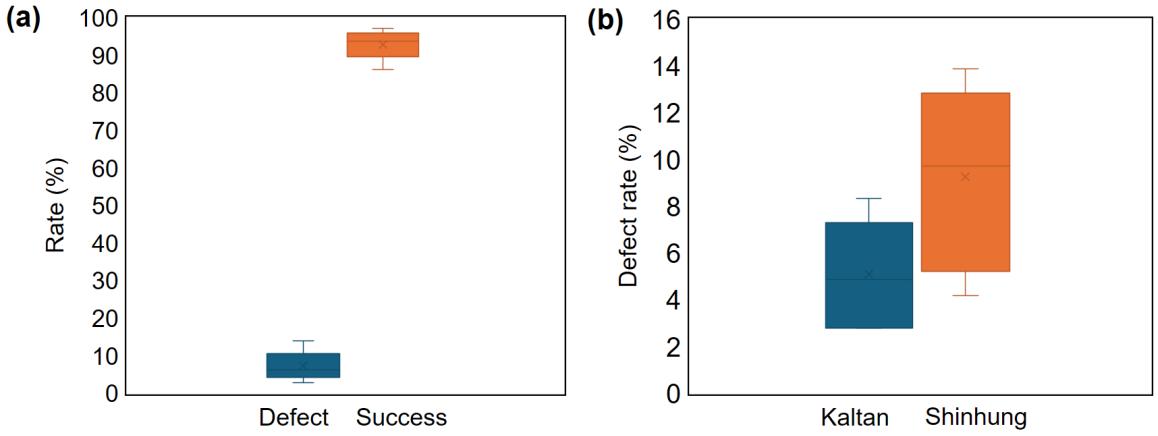


Figure 17. Box–whisker plots of the seedling transplanting performance evaluation: (**a**) defected rate and success rate (%), and (**b**) seedling defected rate (%) per variety.

Planting seedlings at an appropriate depth and maintaining an upright position are critical for promoting effective root–soil contact, which facilitates more efficient root development and nutrient absorption [16]. Uprightness refers to the vertical positioning of

seedlings in the soil, without tilting or leaning to either side. During the seedling planting test, both the upright angle and planting depth were measured across six trays consisting of Trays 1–3 for Kaltan and Trays 4–6 for Shinhung with 31 seedlings sampled per tray. An uprightness angle of 90° represents ideal vertical alignment, while deviations below this value indicate tilt, which may affect seedling anchorage. Mean uprightness angles and their standard deviations (SD) were used to evaluate planting precision and consistency across trays.

As shown in Table 13, the Kaltan cultivar exhibited slightly higher and more uniform planting angles, averaging 82.91 ± 4.70°, 77.87 ± 7.82°, and 80.03 ± 7.22° for Trays 1–3, respectively. These values indicate that Kaltan seedlings were generally well-aligned, which demonstrated the most stable and accurate planting performance.

Table 13. Planting angles (°) within different trays.

Seedling	Kaltan Seedlings (Tray1~3)			Shinhung Seedlings (Tray4~6)		
	Tray1	**Tray2**	**Tray3**	**Tray4**	**Tray5**	**Tray6**
1.	82.1	84.4	82.2	82.4	82.1	80.7
2.	87.8	67.1	71.6	76.6	66.5	88.7
3.	76.9	79.6	83.2	70.9	81.3	68.4
4.	83.7	67.2	79.6	86.5	73.6	85.7
5.	85.6	68.5	80.9	88.6	65.3	64.6
6.	87.1	62.5	74.6	82.4	89.2	87.2
7.	80.7	87.8	75.3	83.8	89.1	81.3
8.	82.3	82.9	84.2	80.9	87.2	81.8
9.	81.7	64.5	86.1	87.4	82.5	73.4
10.	84.3	77.2	64.5	53.6	69.7	79.4
11.	85.5	87.4	72.6	78.5	67.7	87.2
12.	81.9	71.5	79	85.4	85	78.1
13.	85.4	81.1	70.7	80.9	79.7	87.7
14.	76	72.9	86.5	89.5	88.5	89.3
15.	89.5	84.3	88	79.6	67.2	82.3
16.	89	70.3	82.3	83.4	84.2	78.9
17.	87.2	83.6	88.7	83.3	81.7	85.3
18.	83.1	77.6	86.7	85.3	79.6	61.7
19.	83	86.1	87.4	88.6	75.2	75.8
20.	85.8	85.5	77.2	82.5	84.5	79.3
21.	76.5	88.1	65.8	81.7	58.8	83.1
22.	85.3	83.8	87.2	79.7	80.5	88.4
23.	70.3	71.1	69.1	69.6	76.2	81.6
24.	80.1	68.9	71.6	88.1	57.6	65.8
25.	79.3	85.1	85.3	51.4	89.8	79.5
26.	88	83.1	87	75.9	85.5	89.2
27.	81.9	77.2	73.3	75.3	81.5	76.8
28.	73.2	74.5	82.6	82.5	82.5	82.7
29.	82.2	71.6	88.5	68.8	82.2	87.5
30.	85.4	88.2	86.7	86.7	84.3	85.8
31.	89.7	80.6	82.8	86.6	80.1	87.4
Total (Ave. + SD)	82.91 ± 4.70	77.87 ± 7.82	80.03 ± 7.22	79.88 ± 9.12	78.67 ± 8.79	80.79 ± 7.48

In contrast, the Shinhung cultivar (Trays 4–6) recorded mean angles of 79.88 ± 9.12°, 78.67 ± 8.79°, and 80.79 ± 7.48°, showing greater angular variation and slightly lower overall verticality. This variability suggests that Shinhung seedlings were more sensitive to mechanical handling, likely due to differences in stem rigidity and plug cohesion. Such irregularity may also reflect asynchrony between the seedling feeding and planting mechanisms or structural heterogeneity that affects stable placement in the soil. These variations may further indicate differences in seedling structural robustness, which can result in skewed posture, leaning, or curvature factors that adversely affect mechanical transplanting efficiency and initial soil anchorage. A higher dispersion in uprightness angles implies inconsistent performance of the planting mechanism, potentially leading to tilted seedlings that are more prone to desiccation, mechanical instability, or growth asymmetry. Studies and agricultural engineering guidelines commonly regard an upright angle of approximately 90° as the standard for mechanical transplantation of vegetable seedlings, as it ensures stable root-to-soil contact and promotes vertical growth orientation [5]. The overall average planting angle across the six trays was 80.23 ± 7.16°, which is relatively close to the ideal 90°, considered favorable for seedling growth and establishment.

Planting depth is a key agronomic factor influencing root development, anchorage strength, and field establishment of transplanted seedlings. As shown in Table 14, the average planting depths for the Kaltan cultivar ranged from 14.20 ± 4.18 mm (Tray 1) to 38.05 ± 5.62 mm (Tray 3), while for the Shinhung cultivar, depths ranged from 30.01 ± 4.63 mm (Tray 4) to 35.04 ± 5.44 mm (Tray 6). The observed standard deviations (±4.18 to ± 6.11 mm) indicate moderate variation in planting precision among trays. According to previous studies [29,30], the recommended planting depth for pepper seedlings lies between 20 mm and 60 mm. Depths shallower than this range may promote faster shoot emergence but can compromise root anchorage and increase vulnerability to wind and desiccation, as observed in Tray 1 (14.20 ± 4.18 mm). In contrast, the deeper and more uniform planting depths in Tray 3 (38.05 ± 5.62 mm), Tray 4 (30.01 ± 4.63 mm), and Tray 6 (35.04 ± 5.44 mm) fall within or near the agronomic optimum, suggesting better potential for balanced root–shoot development and early establishment.

Table 14. Planting depths (mm) within different trays.

Seedling	Kaltan Seedlings (Tray1~3)			Shinhung Seedlings (Tray4~6)		
	Tray1	Tray2	Tray3	Tray4	Tray5	Tray6
1.	15.2	23.1	41.5	33.6	27.4	38.2
2.	10.8	18.7	35.4	27.2	20.5	30.1
3.	10.4	21.9	42.3	28.9	18.1	36.5
4.	18.7	12.5	31.6	37.8	30.2	33.9
5.	14.3	19.5	39.2	29.8	26.8	35.6
6.	22.6	26.4	47.8	40.1	34.5	46.2
7.	11.6	14.2	34.3	27.1	19.3	40.9
8.	12.3	16.8	36.7	32.9	23.1	32.7
9.	10.9	13.6	28.9	25.2	18.7	25.9
10.	16.9	22.5	41.3	33.1	29.5	39.1
11.	15.6	26.7	48.6	40.4	35.2	40.4
12.	8.5	13.9	34.9	23.6	16.4	34.7
13.	11.2	17.3	34.6	30.7	21.8	32.3
14.	21.4	27.8	43.5	33.8	33.9	41.2
15.	4.6	14.9	25.1	21.9	15.6	24.3
16.	18.2	24.1	39.4	31.5	28.2	34.6
17.	10.9	14.8	31.7	24.8	19.7	32.1
18.	16	20.2	38.9	32.5	25.4	35.9
19.	13.7	17.6	35.8	29.9	22.7	31.5
20.	16.9	28.4	44.2	33.3	32.8	40.1
21.	12.1	16.6	30.5	20.5	14.9	28.4
22.	10.9	14.7	33.6	28.3	20.3	29.8
23.	17.8	25.6	41.9	30.7	21.5	38.4
24.	12.5	18.1	37.4	27.1	26.6	33.6
25.	10.2	15.2	34.8	27.5	22	29.7
26.	23.1	27.4	48.1	29.7	36.1	46.8
27.	13.4	12.9	35.4	25.6	20.8	27.5
28.	18.5	26.2	43.2	30.8	33	40.9
29.	11.8	25.2	38.7	29.4	24.5	33.2
30.	13.6	21.7	39.7	31.8	27.1	35.1
31.	15.9	23.3	40.8	30.9	28.7	36.8
Total (Ave. + SD)	14.20 ± 4.18	20.05 ± 5.10	38.05 ± 5.62	30.01 ± 4.63	25.00 ± 6.11	35.04 ± 5.44

The moderate variability in depth across trays suggests that while the transplanter achieved generally consistent performance, minor deviations may have arisen from factors such as tray geometry, plug height differences, or uneven soil surfaces during operation. Improving depth control precision across trays would further enhance planting uniformity and transplanting efficiency in mechanized pepper production.

Unlike semi-automatic transplanters currently used in Korea that still depend on manual seedling extraction and feeding, the proposed system fully automates both tasks, thereby minimizing labor input and human-induced variation. The reliable seedling deposition performance observed in the field—characterized by a success rate above 92%, defect rate below 10%, and uprightness and planting depth within agronomic tolerance—demonstrates that the newly developed device can maintain planting quality while eliminating the need for additional workers at the rear of the machine. This represents a significant improvement in operational efficiency compared with existing commercial models intended for similar crops.

4. Discussion

This study investigated the kinematic behavior and field performance of a link-driven hopper planting mechanism designed for pepper transplanters under Korean field conditions. The analysis identified the optimal hopper positions during the seedling supply and deposition phases as 320.68 mm and −321.56 mm along the *X*-axis, and 292.63 mm and −617.28 mm along the *Y*-axis, respectively. The corresponding planting trajectory exhibited a width of 166.88 mm, and a height of 318.81 mm. Simulated peak velocities of the hopper were 0.35 m/s (*X*-axis) and 0.47 m/s (*Y*-axis), with peak accelerations of 0.95 m/s^2 and 1.68 m/s^2, respectively. Field trials revealed an overall average upright planting angle of 80.03 ± 7.56°, an average planting depth of 27.06 ± 8.18 mm, a defect rate of 7.18 ± 3.09%, and a success rate of 92.83 ± 3.09%, validating the efficacy of the proposed mechanism under real field conditions.

The optimized crank length of 75 mm enabled the hopper to follow a near-oval trajectory that facilitated smooth vertical motion, enabling synchronized seedling supply and deposition. Deviations in crank length from this optimal value led to reduced planting depth and suboptimal alignment between the seedling and the planting hole, thereby increasing the likelihood of planting defects. Despite minor positional discrepancies along the *X*-axis between simulated and actual hopper trajectories likely attributed to mechanical deflection, linkage backlash, and speed variation, the close alignment along the *Y*-axis demonstrated the robustness of the mechanism in maintaining vertical precision.

Zhao et al. [3] developed a double-planet carrier gear-type transplanter that achieved a transplanting trajectory of 298.05 mm and a success rate of 94.43%. The present study's trajectory height and accuracy closely align with these values, demonstrating that the fundamental principles of link-based motion design, including proper tuning of crank and rocker components, remain applicable across various transplanter architectures and crop types. The velocity and acceleration ranges observed in this study fall well within the thresholds reported in the previous literature for transplanting systems. The peak experimental velocities reached 0.635 m/s at *X*-axis and 0.956 m/s at *Y*-axis, while accelerations were measured up to 2.65 m/s^2 along the *Y*-axis. These values compare favorably to those reported by [21], who documented a maximum planting velocity of 1.032 m/s and an acceleration of 6.51 m/s^2 for a rotary gear-driven transplanter. The moderate acceleration levels in the present study suggest reduced mechanical shocks to the seedlings, contributing to lower defect rates and improved transplanting uniformity.

The measured power requirements of the mechanism ranged from +69.46 W to −76.23 W, which aligns with the recommended operational range (50–150 W) for vegetable seedling transplanters [30]. This low-power demand emphasizes the efficiency of the link-driven mechanical design, which avoids the complexity and energy requirements of sensor-based feedback systems while maintaining adequate performance.

The prototype transplanter demonstrated overall high deposition success, with Kaltan seedlings achieving better performance (94.9% success; 5.1% defects) and more consistently than Shinhung (90.7% success; 9.3% defects), indicating greater sensitivity of the Shinhung cultivar to tray-to-tray variation. Mean planting angles clustered near 80° for both cultivars slightly forward of vertical although Shinhung showed wider angular dispersion, consistent with its higher defect These patterns likely result from cultivar-specific plug and stem mechanics (e.g., plug cohesion and stem rigidity) interacting with release timing and furrow/backfill dynamics, which can shift the plug forward or result in partial seating [22,24]. The achieved average upright planting angle of 80.23° is reasonably close to the ideal 90°, indicating that the seedlings were predominantly planted in a structurally vertical posture. Verticality plays a crucial role in promoting effective root–soil contact, balanced auxin distribution, and uniform

phototropic response, all of which are vital for seedling establishment. This finding agrees with agronomic standards that define uprightness as a key determinant of transplant success [16].

The variance analysis revealed that the pepper seedling variety influenced transplanting performance. Shinhung seedlings showed a higher mean defect rate (9.26%) compared to Kaltan (5.09%), although this difference was borderline non-significant (p = 0.053). However, the significantly larger variance observed in Shinhung (F = 2.94) indicates less uniform mechanical behavior, likely due to differences in plug cohesion and stem rigidity. Since automated transplanting requires a consistent seedling structure for reliable extraction, handling, and deposition, Kaltan demonstrated better compatibility with the proposed mechanism. These results emphasize that seedling quality traits are critical determinants of performance in fully automated transplanting systems, and should be considered in variety selection and machine optimization.

Planting depth is another important parameter, with the observed mean of 27.06 ± 8.18 mm falling within the acceptable agronomic range for pepper cultivation. Trays with planting depths closer to the optimal range showed better field establishment, whereas shallow planting (e.g., Tray 1 at 14.20 ± 4.18 mm) increased the risk of seedling desiccation and mechanical instability. The inconsistency between the seedling supply and hopper operation caused seedling discharge instability, leading to irregular seedling ejection, further influenced by soil hardness within the planting plots. In addition to terrain conditions, improved performance requires redesigning the seedling supply system to maintain consistent and reliable discharge, along with the addition of a manual tray adjustment lever that allows operators to make necessary adjustments in the field, as shown in Figure 18. The average defect rate of 7.17% observed in this study is lower than the rates reported in earlier mechanical transplanting trials without synchronization of hopper motion and seedling supply, further affirming the reliability of the link-driven mechanism. Variation in defect rates among trays may be attributable to uneven ridge formation, seedling morphology differences, or inconsistencies in tray loading and feeding mechanisms.

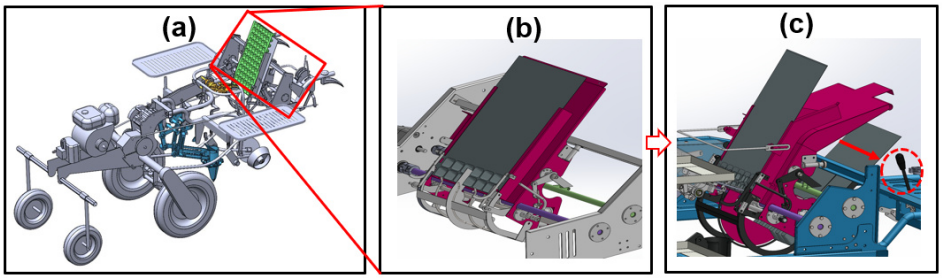


Figure 18. Proposed design improvements: (**a**) prototype design, (**b**) initial seedling supply component, and (**c**) proposed seedling supply with a manual tray adjustment lever.

Numerous studies have emphasized the importance of synchronizing seedling pick-up, conveying, and planting operations to ensure uniform planting depth and uprightness [17,31,32]. The results of the present study confirm that such synchronization can be effectively achieved using a mechanically driven system, thereby reducing dependence on complex electronic controls. While forward speed and crop-specific factors may vary across transplanter designs, the consistency of optimal results in this study with existing research underscores the universality of kinematic modeling and simulation in achieving transplanting efficiency [33,34].

Despite the promising performance of the link-driven hopper mechanism, several limitations were identified. The discrepancies between simulated and experimental hopper positions, especially along the X-axis (~97 mm), indicate mechanical backlash and linkage deflection that affect trajectory accuracy. Variability in planting depth (±9.12 mm) also suggests inconsistencies in furrow formation and soil interaction. Reliance of the mechanism

on purely mechanical synchronization, while cost-effective, limits adaptability to changing seedling morphology or soil conditions. Moreover, evaluation was restricted to two pepper cultivars under uniform field conditions, limiting generalizability. Future work should focus on reducing linkage backlash, incorporating lightweight sensor feedback for real-time trajectory correction, optimizing link geometry through multi-objective algorithms, and validating performance across diverse crops, terrains, and environmental conditions.

5. Conclusions

This study demonstrated the feasibility of a fully automated link-driven hopper mechanism capable of extracting pepper seedlings directly from nursery trays and depositing them precisely into the soil without manual assistance. This eliminates operator dependency common in semi-automatic transplanters and contributes to labor-saving mechanization.

Kinematic analysis using a vector-loop model, combined with simulation and field testing, was conducted to determine the position, velocity, and acceleration characteristics of the hopper throughout the transplanting cycle. The calculated maximum hopper positions were 320.68 mm (X-axis) and -321.56 mm (Y-axis) at seedling supply, and 292.63 mm (X-axis) and -617.28 mm (Y-axis) at soil deposition. Corresponding measured values were 223.67 mm (X-axis) and -326.32 mm (Y-axis) at seedling supply, and 390.55 mm (X-axis) and -645.67 mm (Y-axis) at soil deposition. The comparison confirmed good agreement between calculated and measured trajectories, validating the predictive kinematic model. Simulated hopper velocities ranged from +0.06 to -0.35 m/s (X-component) and +0.47 to -0.45 m/s (Y-component), while measured velocities were +0.43 to -0.63 m/s (X-component) and +0.95 to -0.80 m/s (Y-component). Similarly, calculated accelerations ranged between 0.75 to -0.95 m/s^2 (X-component) and +1.10 to -1.68 m/s^2 (Y-component), whereas measured values reached +1.14 to -1.21 m/s^2 (X-component) and +1.61 to -2.65 m/s^2 (Y-component). These results indicate that the simulated motion closely replicated experimental performance, demonstrating the reliability of the model for motion prediction and design optimization.

Field evaluation indicated that seedling variety affected mechanical transplanting performance. Kaltan seedlings exhibited lower defect rates (5.09 $\pm$ 2.27%) and higher success rates (94.91 $\pm$ 2.27%) than Shinhung (9.26 $\pm$ 3.90% and 90.74 $\pm$ 3.90%). Although the difference in means was borderline significant ($p = 0.053$), variance analysis showed significantly greater variability in Shinhung, suggesting weaker plug cohesion and reduced tolerance to mechanical interaction. These findings highlight the importance of matching seedling morphological quality with automated transplanting systems.

Overall, the planting mechanism achieved an average upright planting angle of 80.03 $\pm$ 7.56°, a mean planting depth of 27.06 $\pm$ 8.18 mm, and a transplanting rate of 24 seedlings min^{-1}, with an overall success rate of 92.83 $\pm$ 3.73% and minimal defect levels as low as 2.77%. Deviations in planting performance were mainly attributed to soil irregularities, tray design, seedling structural differences, and synchronization between seedling release and hopper motion. In contrast to commercially available semi-automatic pepper transplanters in Korea, which require continuous manual assistance for seedling supply, the proposed link-driven hopper mechanism enables a fully automated transplanting process from tray extraction to soil placement. This automation reduces labor requirements, improves planting uniformity, and mitigates the risk of seedling damage caused by inconsistent manual handling. Therefore, the developed mechanism offers practical advantages for mechanized pepper cultivation by enhancing labor efficiency and transplanting consistency, addressing key limitations of existing equipment used in Korean pepper production.

Author Contributions: Conceptualization, E.H. and S.-O.C.; methodology, E.H. and M.N.R.; software, E.H., M.R.A. and S.-H.P.; validation, E.H., D.-H.L., M.R.A., M.N.R., K.-H.L. and S.-H.P.; formal analysis, E.H., K.-H.L. and S.-H.P.; investigation, D.-H.L. and S.-O.C.; resources, S.-O.C.; data curation E.H., M.R.A., M.N.R., K.-H.L. and S.-H.P.; writing—original draft preparation, E.H.; writing—review and editing, M.R.A., M.N.R., K.-H.L., D.-H.L. and S.-O.C.; visualization, E.H., M.N.R., K.-H.L. and D.-H.L.; supervision, S.-O.C.; project administration, D.-H.L. and S.-O.C.; funding acquisition, S.-O.C. All authors have read and agreed to the published version of the manuscript.

Funding: This work was carried out with the support of "Cooperative Research Program for Agriculture Science and Technology Development (Project No. RS-2021-RD009653)", Rural Development Administration, Republic of Korea.

Institutional Review Board Statement: Not applicable.

Informed Consent Statement: Not applicable.

Data Availability Statement: Data contained within the article.

Conflicts of Interest: The authors declare no conflicts of interest.

References

1. Barrett, H.; Rose, D.C. Perceptions of the fourth agricultural revolution: What's In, what's out, and what consequences are anticipated? *Sociol. Rural.* **2022**, *62*, 162–189. [CrossRef]
2. Kumar, A.; Karn, N.; Sharma, H. IoT, AI, and Robotics Applications in the Agriculture Sector. In *Advanced Computational Methods for Agri-Business Sustainability*; IGI Global: Hershey, PA, USA, 2024; pp. 243–272.
3. Zhao, X.; Liao, H.; Ma, X.; Dai, L.; Yu, G.; Chen, J. Design and experiment of double planet carrier planetary gear flower transplanting mechanism. *Int. J. Agric. Biol. Eng.* **2021**, *14*, 55–61. [CrossRef]
4. Zhou, M.; Sun, H.; Xu, X.; Yang, J.; Wang, G.; Wei, Z.; Xu, T.; Yin, J. Study on the method and mechanism of seedling picking for pepper (*Capsicum annuum* L.) plug seedlings. *Agriculture* **2023**, *14*, 11. [CrossRef]
5. Iqbal, M.Z.; Islam, M.N.; Ali, M.; Kabir, M.S.N.; Park, T.; Kang, T.G.; Park, K.S.; Chung, S.O. Kinematic analysis of a hopper-type dibbling mechanism for a 2.6 kW two-row pepper transplanter. *J. Mech. Sci. Technol.* **2021**, *35*, 2605–2614. [CrossRef]
6. Reza, M.N.; Ali, M.; Habineza, E.; Kabir, M.S.; Kabir, M.S.N.; Lim, S.J.; Choi, I.S.; Chung, S.O. Analysis of operating speed and power consumption of a gear-driven rotary planting mechanism for a 12-kW six-row self-propelled onion transplanter. *Span. J. Agric. Res.* **2023**, *21*, e0207. [CrossRef]
7. Khadatkar, A.; Mathur, S.M.; Dubey, K.; BhusanaBabu, V. Development of embedded automatic transplanting system in seedling transplanters for precision agriculture. *Artif. Intell. Agric.* **2021**, *5*, 175–184. [CrossRef]
8. Gobie, W. A seminar review on red pepper (*Capsicum*) production and marketing in Ethiopia. *Cogent Food Agric.* **2019**, *5*, 1647593. [CrossRef]
9. KOSTAT (Statistics Korea). *Production of Chili Pepper, Sesame and Highland Potatoes in 2022*; Ministry of Data and Statistics: Daejeon, Republic of Korea, 2022.
10. RDA (Rural Development Administration of Korea), Department of Agricultural Engineering. *2023 Pepper Mechanization Status in Korea*; Department of Agricultural Engineering: Jeonju, Republic of Korea, 2023.
11. Habineza, E.; Ali, M.; Reza, M.N.; Woo, J.K.; Chung, S.O.; Hou, Y. Vegetable transplanters and kinematic analysis of major mechanisms: A review. *Korean J. Agric. Sci.* **2023**, *50*, 113–129. [CrossRef]
12. Habineza, E.; Reza, M.N.; Bicamumakuba, E.; Haque, M.A.; Park, S.H.; Lee, D.H.; Lee, Y.S. Pepper transplanting mechanisms and kinematic simulation analysis: A review. *Precis. Agric. Sci. Technol.* **2024**, *6*, 17–32. [CrossRef]
13. Zhang, J.; Long, X.; Han, C.; Yuan, P.; Gao, J. Design and experiments of mechanically-driven automatic taking and throwing system for chili plug seedlings. *Trans. Chin. Soc. Agric. Eng.* **2021**, *37*, 20–30.
14. Mudrov, A.P.; Mudrov, A.G.; Yakhin, S.M.; Pikmullin, G.V. Research results of spatial mechanisms and directions of their application in farming machinery. *BIO Web Conf.* **2020**, *27*, 143. [CrossRef]
15. Chowdhury, M.; Reza, M.N.; Ali, M.; Kabir, M.S.N.; Kiraga, S.; Lim, S.J.; Choi, I.S.; Chung, S.O. Vibration assessment of a 12-kw self-propelled riding-type automatic onion transplanter for transplanting performance and operator comfort. *Appl. Sci.* **2023**, *13*, 1927. [CrossRef]
16. Masilamani, P.; Venkatesan, S.; Navamaniraj, K.N.; Rajarathinam, P.; Alagesan, A.; Thiagu, K. Impact of the orientation of seed placement and depth of its sowing on germination: A review. *J. Appl. Nat. Sci.* **2023**, *15*, 314–324. [CrossRef]
17. Yang, Q.; Huang, G.; Shi, X.; He, M.; Ahmad, I.; Zhao, X.; Addy, M. Design of a control system for a mini-automatic transplanting machine of plug seedling. *Comput. Electron. Agric.* **2020**, *169*, 105226. [CrossRef]

18. Landge, R.; Hure, O.; Tambe, G.; Aher, D.; Gadakh, S.; Plate, B. Design and manufacturing of pick and drop system for automatic vegetable transplanter. *Int. Res. J. Eng. Technol.* **2024**, *11*, 1361–1368.
19. Hwang, S.J.; Park, J.H.; Lee, J.Y.; Shim, S.B.; Nam, J.S. Optimization of main link lengths of transplanting device of semi-automatic vegetable transplanter. *Agronomy* **2020**, *10*, 1938. [CrossRef]
20. Zhou, M.; Sun, L.; Du, X.; Zhao, Y.; Xin, L. Optimal design and experiment of rice pot seedling transplanting mechanism with planetary Bezier gears. *Trans. ASAB* **2014**, *57*, 1537–1548.
21. Reza, M.N.; Islam, M.N.; Chowdhury, M.; Ali, M.; Islam, S.; Kiraga, S.; Lim, S.J.; Choi, I.S.; Chung, S.O. Kinematic analysis of a gear-driven rotary planting mechanism for a six-row self-propelled onion transplanter. *Machines* **2021**, *9*, 183. [CrossRef]
22. Liu, J.Z.; Zhao, S.Y.; Li, N.; Faheem, M.; Zhou, T.; Cai, W.J.; Zhao, M.Z.; Zhu, X.Y.; Li, P.P. Development and field test of an autonomous strawberry plug seeding transplanter for use in elevated cultivation. *Appl. Eng. Agric.* **2019**, *35*, 1067–1078. [CrossRef]
23. Reis, Â.V.D.; Forcellini, F.A. Functional analysis in the evaluation of four concepts of planters. *Ciência Rural* **2002**, *32*, 969–975. [CrossRef]
24. Hu, S.; Hu, M.; Yan, W.; Zhang, W. Design and experiment of an integrated automatic transplanting mechanism for picking and planting pepper hole tray seedlings. *Agriculture* **2022**, *12*, 557. [CrossRef]
25. Han, L.; Mao, H.; Hu, J.; Tian, K. Development of a doorframe-type swinging seedling pick-up device for automatic field transplantation. *Span. J. Agric. Res.* **2015**, *13*, e0210. [CrossRef]
26. Abriham, A. Influence of Inter and intra-Row Spacing on Hot Pepper (*Capsicum Annum* L.) Growth, Yield and Yield Component of Under Rain Fed at Guraferda and Gimbo, Southwest Ethiopia. *Int. J. Trends Hortic.* **2024**, *1*, 4–9.
27. RDA (Rural Development Administration of Korea), Department of Agricultural Engineering. *2023 Pepper Planting in Korea*; Department of Agricultural Engineering: Jeonju, Republic of Korea, 2023.
28. Dihingia, P.C.; Prasanna Kumar, G.V.; Sarma, P.K. Development of a hopper-type planting device for a walk-behind hand-tractor-powered vegetable transplanter. *J. Biosyst. Engeering* **2016**, *41*, 21–33. [CrossRef]
29. Paudel, B.; Basak, J.K.; Jeon, S.W.; Lee, G.H.; Deb, N.C.; Karki, S.; Kim, H.T. Development and field testing of biodegradable seedling plug-tray cutting mechanism for automated vegetable transplanter. *J. Agric. Eng.* **2024**, *55*, 1566. [CrossRef]
30. Markumningsih, S.; Hwang, S.J.; Kim, J.H.; Jang, M.K.; Shin, C.S.; Nam, J.S. Comparison of consumed power and safety of two types of semi-automatic vegetable transplanter: Cam and four-bar link. *Agriculture* **2023**, *13*, 588. [CrossRef]
31. Liu, W.; Tian, S.; Wang, Q.; Jiang, H. Key technologies of plug tray seedling transplanters in protected agriculture: A review. *Agriculture* **2023**, *13*, 1488. [CrossRef]
32. Lin, S.; Liu, J.; Wang, H.; Zhang, Y. A novel geometric approach for planar motion generation based on similarity transformation of pole maps. *Mech. Mach. Theory* **2018**, *122*, 97–112. [CrossRef]
33. Wu, K.; Chen, J.; Lou, J.; Yu, Y.; Li, J. Design and parameters optimization of pteris vittata automatic sowing machine for phytoremediation. *Int. J. Eng.* **2020**, *33*, 694–701. [CrossRef]
34. Zhang, S.; Xia, J.; Zhou, Y.; Wu, D.; Cao, C.; Xia, P. Field experiment and seeding performance analysis of pneumatic cylinder-type precision direct seed-metering device for rice. *Trans. Chin. Soc. Agric. Eng.* **2017**, *33*, 14–23.

Disclaimer/Publisher's Note: The statements, opinions and data contained in all publications are solely those of the individual author(s) and contributor(s) and not of MDPI and/or the editor(s). MDPI and/or the editor(s) disclaim responsibility for any injury to people or property resulting from any ideas, methods, instructions or products referred to in the content.